JPRS L/9856

20 July 1981

USSR Report

PHYSICS AND MATHEMATICS

(FOUO 7/81)

FBIS FOREIGN BROADCAST INFORMATION SERVICE

NOTE

JPRS publications contain information primarily from foreign newspapers, periodicals and books, but also from news agency transmissions and broadcasts. Materials from foreign-language sources are translated; those from English-language sources are transcribed or reprinted, with the original phrasing and other characteristics retained.

Headlines, editorial reports, and material enclosed in brackets [] are supplied by JPRS. Processing indicators such as [Text] or [Excerpt] in the first line of each item, or following the last line of a brief, indicate how the original information was processed. Where no processing indicator is given, the information was summarized or extracted.

Unfamiliar names rendered phonetically or transliterated are enclosed in parentheses. Words or names preceded by a question mark and enclosed in parentheses were not clear in the original but have been supplied as appropriate in context. Other unattributed parenthetical notes within the body of an item originate with the source. Times within items are as given by source.

The contents of this publication in no way represent the policies, views or attitudes of the U.S. Government.

APPROVED FOR RELEASE: 2007/02/09: CIA-RDP82-00850R000400030037-4

JPRS L/9856

20 July 1981

USSR REPORT

PHYSICS AND MATHEMATICS

(FOUO 7/81)

CONTENTS

CRYSTALS AND SEMICONDUCTORS

UDC 535.51

CURRENT PROBLEMS IN ELLIPSOMETRY

Novosibirsk SOVREMENNYYE PROBLEMY ELLIPSOMETRII in Russian 1980 (signed to press 10 Nov 80) pp 2-3, 185-186

[Annotation, editor's preface and table of contents from book "Current Problems in Ellipsometry", edited by Anatoliy Vasil'yevich Rzhanov, Institute of Physics of Semiconductors, Siberian Department, USSR Academy of Sciences, Izdatel'stvo "Nauka", 1400 copies, 186 pages]

[Text] This collection is devoted to research dealing with the main areas of development of ellipsometry and its applications. The papers examine an extensive class of problems in this promising field of science--from the theoretical aspects of the reflection of light to the development of various types of ellipsometers designed for the practical requirements of semiconductor microelectronics.

Intended for experimental physicists and technological engineers working in the field of physical electronics, surface physics and chemistry and the physics of semiconductors.

From the Editor

According to convention established over the last 10-15 years, the term "ellipsometry" denotes an optical technique of studying the state of a surface and determining (measuring) the parameters of thin films based on analysis of the change in state of polarization of a light beam upon reflection.

There are two factors that make ellipsometric measurements particularly attractive. In the first place, they are not only non-contact and non-destructive, but also "non-disturbing" to the investigated system under condition that the wavelength and intensity of the light are properly selected. This feature enables ellipsometric measurements directly in the course of the given process, high temperature of the surface of the specimen and aggressiveness of the ambient medium being no problem.

In the second place, the state of polarization of the reflected light is quite sensitive to minimum changes of surface state and parameters of thin-film systems. For example the best ellipsometers can fix changes in the adsorption coating of a surface of the order of thousandths of a monolayer.

Since processes on phase interfaces and in thin-film systems are becoming a research topic in many fields of natural science and technolgy (in the physics and physical chemistry of surfaces, microelectronics, science of materials and metallurgy, optics and mechanics, biology and medicine, atomic and genetic engineering), it is understandable why there has been a recent upsurge of interest in ellipsometry with its unusual capabilities.

The First All-Union Conference on Ellipsometry as a Method of Studying Physicochemical Processes on the Surface of Solids was held in June of 1977 at Akademgorodok in the Novosibirsk Science Center of the Siberian Department of the USSR Academy of Sciences. This collection contains the most interesting papers delivered at that conference.

Contents page

6610
CSO: 1862/183

FLUID DYNAMICS

UDC 533.9.15+537.52.7

PROPAGATION OF A SLOW LUMINOUS AIR COMBUSTION WAVE IN A NEODYMIUM LASER BEAM

Moscow KVANTOVAYA ELEKTRONIKA in Russian Vol 8, No 4(106), Apr 81 pp 751-759

[Article by I. A. Bufetov, A. M. Prokhorov, V. B. Fedorov and V. K. Fomin, Physics Institute imeni P. N. Lebedev, USSR Academy of Sciences, Moscow]

[Text] An investigation is made of large-scale propagation and maintenance of an optically thin laser plasma of atmospheric air in the slow combustion mode on a length of up to 20 cm for a duration of ~5 ms by means of a neodymium laser with emission energy of 8 kJ. An optical discharge is achieved for the first time in the slow combustion mode with steady-state pattern of gas movement. A model is proposed for describing the gas dynamics of discharge propagation in which the ratio of the observed velocity to the velocity of movement of the discharge through a quiescent gas is equal to the ratio of velocities of sound in the discharge and in a cool gas. Measurements are made of the velocities of wavefront propagation and the coefficient of absorption of the discharge plasma. Thresholds of induced initiation and propagation of a luminous air combustion wave are determined.

1. Introduction

Slow combustion of an optical discharge in a laser beam was discovered in 1969. Experiments of Ref. 1 done in atmospheric air demonstrated induced initiation, subsonic propagation and prolonged maintenance of an optical discharge plasma by the emission of a neodymium laser operating in the free lasing mode. Initiation of the discharge at a laser radiation intensity much lower than the optical breakdown threshold was achieved by inoculating the laser beam with an absorbing plasma produced by an auxiliary electric discharge. After discharge ignition by laser radiation absorption, the plasma propagated forward and back along the laser beam at subsonic velocity, filling the caustic surface of the focusing lens symmetrically relative to the initiation point. The optical thickness of the plasma on a wavelength of 1.06 μm was small. Discharge plasma propagation in the laser beam was interpreted, as in slow chemical combustion, on the basis of a thermal conductivity mechanism of energy transfer. In calculating the observed velocity of discharge propagation, consideration was taken of the expansion of gas in the combustion front by analogy with chemical combustion from the closed end of a tube.

It should be noted that the use of an inoculating plasma for induced initiation of luminous detonation was proposed in 1968 in Ref. 11. In that same year, Ref. 12 discussed rf discharge in a gas through an induction coil as a slow combustion process. At the same time, propagation of a microwave plasma in a waveguide that had been described in 1961 [Ref. 13] was not interpreted on the basis of a slow combustion mechanism until 1971 [Ref. 14] after the research of Ref. 1-3.

A distinguishing procedural feature of the experiments of Ref. 1 was the similarity of the experimental situation to the simplest case from the standpoint of theory of propagation of a weakly absorbing optical discharge in a beam with cylindrical symmetry. This peculiarity is associated with the use of a powerful laser in Ref. 1, with a power level permitting the use of a lens with small relative apoerture for focusing. Apparently this feature was the reason that subsequent theoretical calculations [Ref. 2-6] were verified by the authors on the basis of the experimental material of Ref. 1. We are referring to a uniform model of motion of the discharge front and to calculation of the threshold conditions, derivation of a formula for the rate of propagation of the discharge with consideration of the threshold [Ref. 2-4] and also to accounting for the influence that radiative thermal conductivity in the ultraviolet part of the spectrum of the self-radiation of the discharge has on motion of the ionization front [Ref. 5, 6].

Our research continues the experiments of Ref. 1 with a number of important changes. Our analysis of the data of Fig. 3 in Ref. 1 showed that the velocity of the discharge front from time $t = 0.4$ ms after the onset of the laser pulse to t=1 ms decreases monotonically from 30 to 10 m/s. (On this time segment we can obviously disregard the influence that gas movement caused by energy release in the initiating electric discharge has on V. Actually, according to the theory of a point explosion [Ref. 15] the corresponding characteristic time of attenuation of perturbations caused by energy release is $t_0 = E^{1/3}\rho^{1/2}p^{-5/6}$ (ρ is density, p is pressure of the medium, E is energy), which for atmospheric pressure and $E = 100$ J gives $t_0 = 0.36$ ms.) The observed velocity reduction can be attributed to two causes: a fairly rapid drop in time in the power of the radiation feeding the discharge, and also the short duration of the laser pulse, during which the velocity of motion of the front does not have time to reach the steady state. To obtain the stationary gasdynamic pattern of laser plasma propagation in the slow combustion mode, we made the following corrections in the conditions of the experiment of Ref. 1: increased the laser pulse duration to 5 ms with a corresponding increase in the energy of the laser facility; made the emission power close to constant over a longer part of the laser pulse duration; eliminated the spike modulation that occurred in Ref. 1. These experiments for the first time gave an optical discharge in the slow combustion mode with steady-state pattern of gas movement in the discharge. To describe the influence that expansion of the gas heated in the combusion front had on the observed rate of motion of the front, in addition to the previously used model of combustion from the closed end of a tube, a model was proposed with a better fit to the conditions of steady-state gas dynamics of the discharge, taking consideration of the motion of hot gas behind the combustion front.

2. Experimental Results

Our experiments were done on a laser stand with emission parameters about an order of magnitude higher than in the first experiments [Ref. 1].

The main laser that maintained the discharge was a neodymium glass unit with energy of up to 8 kJ and radiation pulse duration of 5 ms at the base. An oscillogram of the lasing pulse is shown in Fig. 1 [photo not reproduced]. The lasing pulse was smooth. The spikeless lasing structure was achieved by using a master laser with stable cavity close to confocal, and by minimizing the feedback between amplifier and laser due to scattering by the optical elements. The main laser beam was focused by a lens with focal length of 1 m. The length of the caustic curve determined by the relation $R \leqslant \sqrt{2}R_{min}$ (R is beam radius) was 13.6 cm, the diameter of the spot at the narrow point being $2R_{min} = 4.2$ mm. To measure the energy distribution over the beam cross section in the caustic of the lens, part of the radiation was diverted to a lens identical to that focusing the main beam. I-1070 photographic film was placed at different cross sections in the caustic of this lens. Densitometry of the resultant spots showed how beam diameter in the caustic of the lens depended on distance. Radiation intensity was approximately constant over the cross section at distances of ±8 mm from the focus. Deviation of intensity from the average value in each cross section did not exceed 25%. Optical discharge was initiated by using the plasma produced by breakdown of atmospheric air in the pulse of an auxiliary Q-switched neodymium laser (ignition pulse duration 10^{-7} s, energy 2 J). The ignition pulse was focused by a lens with focal length of 0.25 m onto the caustic of the main laser beam perpendicular to its axis. Luminescence duration of the plasma of the igniting spark was $6 \cdot 10^{-5}$ s; the size of the luminescent region along the caustic of the millisecond laser was 0.5 cm, and in the transverse direction--1.5 cm.

The optical discharge in atmospheric air was ignited as a result of the plasma of the initiating breakdown being "grabbed" by the radiation of the main laser. The threshold of grabbing of the breakdown spark with initiation in the focus of the main beam was $P_g \approx 0.5 \cdot 10^6$ W (with respect to power) and $I_g \approx 4 \cdot 10^6$ W/cm^2 (with respect to intensity). Threshold conditions of the experiment were taken as those in which a plasma luminescence time of 1.5 ms was twice the duration of the ignition spark luminescence; the dimension of the plasma formation along the caustic of the main beam in this case was 1 cm. At a power of twice the threshold value, a discharge was observed to develop with dimensions of ~0.1 m along the caustic. The time of existence of the discharge was limited by the duration of the lasing pulse. At a maximum output energy of the main laser $E = 8.3 \cdot 10^3$ J in the given experiments, the region occupied by the discharge extended for 0.2 m along the beam at a diameter of the luminescent region of 2 cm in the middle part of the spark. The spark was somewhat asymmetric relative to the ignition point. At the end of the lasing pulse, the length of the spark in the direction toward the laser was about 10% greater than in the direction away from the laser. A time-integrated photograph of the spark is shown in Fig. 2 [photo not reproduced].

Time development of the spark was studied by high-speed photography. The observations were made in the direction perpendicular to the plane of the rays of the main and ignition lasers. The pattern of formation and development of the spark is illustrated by single-frame scanning of the process in Fig. 3 [photo not reproduced] and may be described briefly as follows. After breakdown of the air by the ignition laser pulse, the spark begins growing to both sides along the main laser spark. Leading (closer to the laser) and trailing combustion fronts are formed. At the same time, plasma luminescence is quenched at the point of initiation within a time of ~10^{-4} s, which is approximately equal to the time of existence

of the ignition spark plasma. The dimension of the nonluminescent region on the axis of the main laser corresponds approximately to the dimension of the initiating plasma. The discharge is torn into two parts. Two internal fronts are formed and propagate toward each other at velocity $V \approx 5$ m/s, leading to merging of the two halves of the spark at the end of the first millisecond. By the end of this first stage of spark development ($\sim 10^{-3}$ s from the instant of ignition) the dimensions of the spark in the longitudinal direction are slightly greater than its diameter. Then in the second stage there is a nearly symmetric increase in the length of the spark due to advancement of the leading and trailing combustion fronts. The dimensions of the luminescent region in the transverse dimension even immediately behind the combustion front are much greater than (up to double) the diameter of the laser beam, which is a consequence of the rapid lateral dispersal of the gas being heated in the front. Then as the combustion front moves further from the given cross section of the spark the transverse size of the spark continues to grow over the entire lasing pulse, but now at a rate that is dozens of times slower.

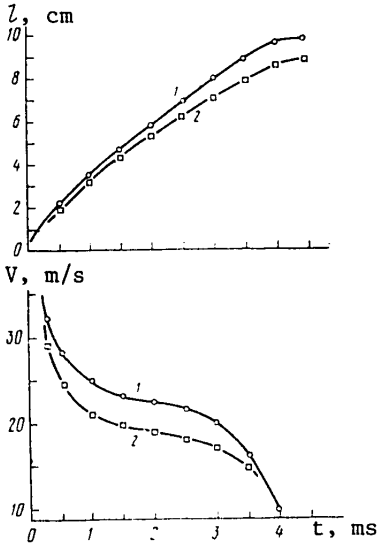

Fig. 4.. Distance traveled by the leading (1) and trailing (2) fronts (top) and velocity of the fronts (bottom) as a function of time (pulse energy E = 8.3 kJ)

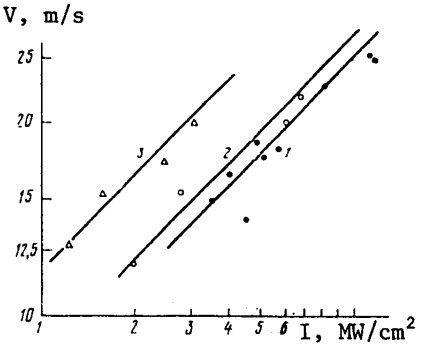

Fig. 5. Velocity of spark front as a function of radius of the front $R \approx 2.2$ (1), 2.8 (2) and 4.2 (3) mm. Straight lines correspond to relation $V \sim I^{\frac{1}{2}}$

The rates of propagation of the spark fronts were measured. From experiment to experiment there was a variation in the energy of the laser pulse and the place of initiation of the discharge relative to the focus of the main beam. In different groups of experiments the spark was initiated at the focus, and at 4 cm and 8 cm to either side of the focus. The distance traveled by the spark front was determined as a function of time from photographs taken in the continuous scanning mode. The time dependence of the rates of propagation of the fronts was found after differentiation. Typical curves are shown in Fig. 4. It can be seen that during the first millisecond there is a rapid reduction in the velocity of advancement of the front from several tens to about 20 m/s. Then for ~2.5 ms (up to collapse of the lasing pulse) there is a comparatively slow change in propagation rate. This corresponds to the two qualitatively different stages in spark development noted earlier. Fig. 5 shows the rates

of propagation of spark fronts for different intensities of radiation incident on the front and different diameters of fronts. An increase is observed in the velocity of the front both with increasing intensity and fixed diameter of the front and for a given intensity as the diameter increases.

In this series of experiments, no special study was done on the threshold of discharge propagation corresponding to zero velocity of the front. However, one can conclude from the available data that the propagation threshold at least does not exceed $0.44 \cdot 10^6$ W with respect to power, and $6 \cdot 10^5$ W/cm^2 with respect to intensity when the radius of the front is $R \approx 0.48$ cm. On the other hand, in our experiments at $P \approx 0.5$ MW in the cross section with $R = 0.2$ cm (focus of the main beam) the velocity of the front $V = 13.5$ m/s. Thus the threshold of propagation is apparently lower than the threshold of grabbing, which for the same radius of $R = 0.2$ cm is ~0.5 MW, as was pointed out above.

The coefficient of absorption of the discharge plasma was measured. Two FD-3 photodiodes were used to determine the time dependence of the percentage of laser radiation transmitted through the spark plasma. Part of the radiation from the laser output was fed to one of the photodiodes. Part of the radiation transmitted through the discharge plasma was focused on the other photodiode. The focusing system collected the transmitted radiation in a solid angle of $\Omega_2 = 30$ msr. The solid angle in which the transmitted radiation would have propagated in the absence of effect of refraction and scattering is $\Omega_1 = 3.6$ msr. The photodiodes were shielded from spurious background illumination by silicon filters. To average out the slight spike structure of the lasing pulse, the signals from both photodiodes were integrated with a time constant of 10 μs and fed to the inputs of an S8-2 two-beam oscilloscope (Fig. 1) [photo not reproduced]. The relative amplitude of the signals from the photodiodes was calibrated in each experiment with respect to the initial part of the lasing pulse at instants preceding the instant of feeding in the ignition spark. The percentage of the transmitted radiation was determined from the ratio of the signals from the photodiodes with consideration of calibration. Comparison of these measurements with the time dependence of spark length enabled determination with time resolution of the coefficient of absorption α of the spark plasma averaged with respect to the length of the spark. The value of α determined in this way remained constant within the limits of accuracy of the measurements (20%) over an interval of 1-3.5 ms from the instant of initiation. Values of $\alpha = 0.03$ and 0.02 cm^{-1} were found at a laser pulse power in the maximum of $P = 1$ MW ($E = 4$ kJ) and 2 MW ($E = 8$ kJ). Let us note that a much lower value of $\alpha = 0.007$ cm^{-1} was found in Ref. 1 in atmospheric air at laser emission powers close to ours. This difference may be due to understatement of α due to failure to account for the change in the length of the discharge with time and disregard of the influence that the initiating plasma has on the absorption being measured. Besides, it is difficult to say what differences in the actual plasma parameters may result from near 100% (in contrast to our experiments) spike modulation of the laser emission.

3. Calculating the Velocity of Motion of the Optical Discharge Front

To describe the propagation of the optical discharge front in the slow combustion mode, Ref. 2, 3 proposed a one-dimensional model in which (in a coordinate system fixed to the front) the equation for the heat flux potential $\Theta = \int_0^T \varkappa(T)\,dT$ becomes

$$\rho_0 u \frac{c_p(\Theta)}{\varkappa(\Theta)} \frac{d\Theta}{dx} = \frac{d^2\Theta}{dx^2} + F_c(\Theta), \qquad (1)$$

where $c_p(\Theta)$ is heat capacity at constant pressure, ρ_0 is the density of the cold gas, $\kappa(\Theta)$ is the coefficient of thermal conductivity, T is temperature, $F(\Theta)$ is the function of the heat sources, $F(\Theta) = I\alpha(\Theta) - A\Theta/R^2 - \Phi(\Theta)$ (the term $A\Theta/R^2$ accounts for thermal conductivity heat losses as a consequence of nonuniformity of the actual problem), $\Phi(\Theta)$ are losses of energy to radiation. The X-axis is directed along the beam, discharge propagates with velocity u in the direction of negative values of x. Let us use equation (1) to get a simple approximate expression for velocity u. Far from the combustion front the heat flux $d\Theta/dx$ approaches zero, always remaining positive, and therefore at a certain value of x_m (and corresponding Θ_m, T_m) it reaches a maximum. At $x = x_m$, $d^2\Theta/dx^2 = 0$, and from (1) we get

$$\left.\frac{d\Theta}{dx}\right|_{x=x_m} = \frac{F(\Theta_m)\,\varkappa(\Theta_m)}{\rho_0 u c_p(\Theta_m)}.$$

An "absorption step" model was considered in Ref. 3, 4 ($\alpha = 0$ at $\Theta < \Theta_1$, $\alpha = \text{const}$ at $\Theta > \Theta_1$; it was assumed besides that the ratio $c_p(T)/\varkappa(T)$ is constant), and in this framework the heat flux reached its maximum value at Θ_1. In this model T_1 (corresponding to Θ_1) plays the part of the "ionization temperature": T_1 = 12,000-14,000 K for absorption of neodymium laser emission in air at atmospheric pressure. By analogy with this model we will also assume that T_m corresponds to the "ionization temperature"--the region of abrupt change in $\alpha(T)$, although this approximation in accounting for radiative thermal conductivity, according to Ref. 5, 6 is less reliable, since $\kappa(T)$ in this case is more strongly dependent on temperature. In all further estiamtes we will assume that $T_m \approx 12{,}000$ K. The difference of the given quantity from that indicated in Ref. 3, 4 can be explained by the fact that we are using the values of $\alpha(T)$ given in Ref. 7 for calculations.

Cross section x_m can be considered the boundary between the working zone of the wave and the zone of heating [Ref. 3]. In the case where the radiation intensity is much greater than the threshold value, the quantity $F(\Theta)$ can be disregarded in (1) at $x < x_m$, and

$$\left.\frac{d\Theta}{dx}\right|_{x=x_m} = \rho_0 u w(\Theta_m),$$

where $w(\Theta)$ is the specific enthalpy of the gas. Equating the values of heat flux obtained above, we get

$$u = \frac{1}{\rho_0}\sqrt{\left.\frac{\varkappa(\Theta)F(\Theta)}{w(\Theta)c_p(\Theta)}\right|_{\Theta=\Theta_m}}. \qquad (2)$$

In order to convert from u to the rate of discharge propagation in the laboratory coordinate system, it is necessary to account for the movement of the cold gas ahead of the front due to expansion of the gas heated in the combustion front. In Ref. 1 this was done in analogy with propagation of the combustion front from the closed end of a tube. In this case, the gas behind the front does not move, and the observed velocity V in accordance with conservation of the flux of material is greater than velocity u:

$$V = u\rho_0/\rho_f \qquad (3)$$

(ρ_0 and ρ_f are respectively the density of the cold gas ahead of the front, and of the hot gas behind the combustion front). Actually, a situation close to combustion from the end of a closed pipe is realized in our experiments on the first stage of discharge development when the leading and trailing fronts are no further from each other than the diameter of the front. As the length of the spark increases the movement of the hot gas behind the wavefront becomes appreciable. In this case, calculation of the velocity V of motion of the front in the laboratory system of coordinates at known u necessitates consideration of the perturbation of the entire mass of the gas entrained in motion both ahead of the wavefront and behind it.

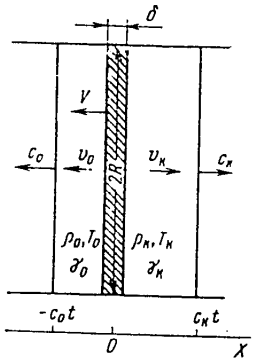

Fig. 6. Diagram of combustion front propagation in an infinite tube

Under the conditions of our experiment, the solution is simplified by the following considerations. In the first place there are homogeneous regions filled with cold gas and hot gas ahead of the combustion front and behind it respectively at distances $d \gg R$. Secondly, due to an absence of inhomogeneities the perturbation waves that arise in the vicinity of the combustion front after reflection from remote obstacles practically do not reach the front. On the first stage of discharge development, where $l \sim R$, the zone of collision of the gas streams from the leading and trailing combustion fronts plays the part of such an inhomogeneity that influences the movement of the flows of heated gas. And in the third place the thickness of the combustion front is less than the diameter of the front, $\delta < 2R$, i. e. the movement of the gas in the vicinity of the front in a certain approximation can be considered uniform. In this connection, the thickness of the front is understood to mean the dimension of the region along the X-axis that covers the greater part of the drop from the initial temperature T_0 to the final temperature T_f. For example calculations according to (1) show that with propagation of a combustion wave in air at a velocity $u = 1$ m/s, there is an increase in temperature from room level to 12,000 K, i. e. by a factor of 40, at a distance of ~1.5 mm; from there the temperature rises to $T_f \sim 18{,}000$ K (a factor of 1.5) over a much greater distance of the order of 1 cm.

This allows us to take the one-dimensional problem of propagation of a combustion through an infinite tube (Fig. 6) as a model problem for determining V, assuming that the region $x < 0$ is filled with the cold gas (with parameters c_0--speed of sound, γ_0--adiabatic exponent), and the region $x > 0$ is filled with hot gas with parameters ρ_f, c_f, T_f, γ_f that coincide with the parameters of the gas after passage of the discharge wave. Let the wave begin propagating at velocity u through the cold gas at time $t = 0$. Then as a consequence of expansion of the gas, compression waves will begin to propagate in both directions with gas velocities v_0 and v_f. The regions covered by the motion are limited by shock waves in analogy with the problem of piston movement in an infinite tube with initially quiescent gas [Ref. 8]. Since $u \ll c$, the pressure differentials can be disregarded, and we can take the shock waves as weak and propagating with corresponding sonic velocities. By using the law of conservation of flux of material through the surface of the combustion front $\rho_0 u = \rho_f (v_f + V)$ and the law of conservation of momentum (taking $V \ll c_0, c_f$),

$\rho_0 v_0 c_0 t = \rho_f v_f c_f t$, and also considering that $v_0 = V - u$, we determine V with accuracy to quantities $\sqrt{\rho_f/\rho_0}$:

$$V = uc_f/c_0 = u\sqrt{\gamma_f \rho_0/\gamma_0 \rho_f},$$
$$v_0/v_f = \rho_f c_f/\rho_0 c_0 = \sqrt{\gamma_f \rho_f/\gamma_0 \rho_0} \ll 1, \quad (4)$$

which is considerably different from result (3) used in Ref. 1. The experimentally determined V may be less than (4) due to disturbance of homogeneity of the gas expansion. The opposite effect is produced by the influence of the gas flow moving from the second combustion front.

4. Discussion of the Results and Conclusion

Thus on the basis of these results the pattern of propagation of an optical discharge in our experiments is as follows. When the inoculating plasma of the optical breakdown is grabbed by the main radiation, an optical discharge is formed with two fronts propagating forward and backward along the laser beam. If we do not consider the time segment when the shock wave that arises as a result of breakdown has an influence on discharge propagation (~100 μs for the given parameters of the initiating spark), it can be assumed that the discharge fronts propagate due to heat-conduction energy transfer with some velocity u relative to the cold gas ahead of the front.

On the first stage, when the radius of the front R is great compared with discharge length l, the movement of the front in the laboratory coordinate system due to the expansion of gas takes place as in the case of combustion from the closed end of a tube [Ref. 1] at velocity $V = u\rho_0/\rho_f$. As l increases there is a reduction in the influence of the second combustion front as a factor that limits the free expansion of the hot gas, leading to a reduction in the observed V. Finally, upon satisfaction of the condition $R \ll l$, the pattern of movement of the gas in the region of the discharge front takes on a steady-state appearance. The rate of propagation is stabilized. In this case the influence of the second front on the rate of propagation can be disregarded, and the motion of the wavefront can be treated within the framework of the model of combustion in an infinite tube. Consequently, the velocity corresponding to an approximately horizontal section in Fig. 4 is determined by expression (4). The abrupt drop in V at the end of the pulse can be explained by a fall-off in the laser emission power.

To estimate u, we use expression (2) where the coefficient of thermal conductivity κ is equal to the sum of the coefficients of ordinary and radiative thermal conductivity [Ref. 5, 6]; $w(T_m)$ and $c_p(T_m)$ are determined from tables [Ref. 7, 9]. For a radiation intensity of $3 \cdot 10^6$ W/cm^2, the corresponding value is u = 1.9 m/s. The final temperature T_f in the discharge can be estimated from the measured value of the coefficient of absorption α. Considering that T_f is on the falling branch of the dependence $\alpha(T)$ (which is confirmed by analysis of heat release and losses in the discharge when the threshold intensity is considerably exceeded), according to Ref. 7 $\alpha = 0.02$-0.03 cm^{-1} corresponds to a temperature $T_f = 17{,}000$-$19{,}000$ K. After substituting $c_f(T_f)$ in (4), we get $V \approx 30$ m/s, which agrees satisfactorily with the measured value V = 20 m/s. Experimental curves for V(I) at a fixed radius of the front R have the form $V \sim I^{1/2}$, which is in agreement with expression (2).

The relation $V \sim R^{0.7-0.6}$ observed in the experiment shows the appreciable influence of two-dimensionality of the actual pattern of combustion front propagation, which can apparently be represented in the form of two effective factors. The first factor is associated with radiative and heat-conduction losses of energy from the plasma column through the lateral surface and is approximately accounted for by introducing a term of the form $A\Theta/R^2 + \Phi$ in equation (1) [Ref. 2-4]. At intensities far from the threshold, as was the case in most of our experiments, the influence of this term is small, and numerical estimates show that it does not give such a strong dependence on radius. The outflow of mass reduces the gasdynamic factor that accounts for motion of the cold gas ahead of the front, and leads to a reduction in the observed V as compared with that calculated by formula (4). At a fixed intensity, and consequently a fixed thickness of the front, the fraction of the mass of gas flowing out through the lateral surface decreases with increasing radius of the front (the situation approaches homogeneity). This is apparently what leads to the increase in velocity of propagation of the front with increasing radius as observed in the experiment. The numerical values of the velocity in this case should approach the values calculated by formula (4).

Thus the experiments done in this research showed a change in the nature of propagation of a slow comubstion front from the mode of burning from the closed end of a pipe to the mode of combustion in an infinite tube. This observed change of conditions is evidence of the appreciable influence that the movement of gas in the discharge region has on the velocity of propagation of the front in the laboratory system of coordinates. A model is proposed, and an estimate is made of the velocity of the combustion front for the second mode. The measured velocity of motion of the combustion front agrees satisfactorily with numerical estimates.

In conclusion, let us consider for a moment the results of Ref. 10 in the part that is pertinent to our own work. In the experiments of Ref. 10 with a CO_2 laser uder conditions of sharp focusing of radiation, the measured velocities of the leading edge that is optically dense on the wave of the supporting discharge radiation vary from 20 to 0.2 m/s. A comparison of experimental velocities with values obtained by solving the unsteady heat conduction equation showed agreement in a range of 3.5-0.2 m/s without consideration of gas movement in the discharge (see (3) and (4) in section 3 of this paper). The small influence of gas dynamics on the rate of discharge propagation in the laboratory coordinate system under the conditions of Ref. 10 can be attributed to the fact that at the given velocities the thickness of the combustion front is greater than or on the order of the diameter of the focused beam, and consequently the pattern of dispersal of the heated gas is essentially two-dimensional.

REFERENCES

1. Bunkin, F. V., Konov, V. I., Prokhorov, A. M., Fedorov, V. B., PIS'MA V ŽHURNAL EKSPERIMENTAL'NOY I TEORETICHESKOY FIZIKI, Vol 9, 1969, p 609.

2. Rayzer, Yu. P., PIS'MA V ZHURNAL EKSPERIMENTAL'NOY I TEORETICHESKOY FIZIKI, Vol 11, 1970, p 195.

3. Rayzer, Yu. P., ZHURNAL EKSPERIMENTAL'NOY I TEORETICHESKOY FIZIKI, Vol 58, 1970, p 2127.

4. Rayzer, Yu. P., "Lazernaya iskra i rasprostraneniye razryadov" [The Laser Spark and Discharge Propagation], Moscow, Nauka, 1974.

5. Boni, A. A., Su, F. Y., PHYS. FLUIDS, Vol 17, 1974, p 340.

6. Su, F. Y., Boni, A. A., PHYS. FLUIDS, Vol 19, 1976, p 960.

7. Biberman, L. M., ed., "Opticheskiye svoystva goryachego vozdukha" [Optical Properties of Hot Air], Moscow, Nauka, 1970.

8. Landau, L. D., Lifshits, Ye. M., "Mekhanika sploshnykh sred" [Mechanics of Continuous Media], Moscow, GITTL [Gosudarstvennoye izdatel'stvo tekhnicheskoy i teoreticheskoy literatury], 1954, p 440

9. Predvoditelev, A. S., Stupochenko, Ye. V., Pleshakov, A. S., Samuylov, Ye. V., Rozhdestvenskiy, I. B., "Termodinamicheskiye funktsii vozdukha" [Thermodynamic Functions of Air], Moscow, Izdatel'stvo vychislitel'nogo tsentra Akademii nauk SSSR, 1962.

10. Kozlov, G. I., PIS'MA V ZHURNAL TEKHNICHESKOY FIZIKI Vol 4, 1978, p 586.

11. Rayzer, Yu. P., PIS'MA V ZHURNAL EKSPERIMENTAL'NOY I TEORETICHESKOY FIZIKI, Vol 7, 1968, p 3.

12. Rayzer, Yu. P., ZHURNAL PRIKLADNOY MATEMATIKI I TEKHNICHESKOY FIZIKI, No 3, 1968, p 3.

13. Beust, W., Ford, W. L., MICROWAVE JOURNAL, Vol 4, No 10, 1961, p 91.

14. Rayzer, Yu. P., ZHURNAL EKSPERIMENTAL'NOY I TEORETICHESKOY FIZIKI, Vol 61, 1971, p 222.

15. Sedov, L. I., "Metody podobiya i razmernosti v mekhanike" [Scaling Theory and Dimensional Analysis in Mechanics], Moscow, Nauka, 1967, p 264.

6610
CSO: 1862/189

LASERS AND MASERS

UDC 539.1

OPTICAL CAVITIES AND THE PROBLEM OF DIVERGENCE OF LASER EMISSION

Moscow OPTICHESKIYE REZONATORY I PROBLEMA RASKHODIMOSTI LAZERNOGO IZLUCHENIYA in Russian 1979 (signed to press 29 Oct 79) pp 2-5, 9-18

[Annotation, introduction and table of contents from book "Optical Cavities and the Problem of Divergence of Laser Emission", by Yuriy Alekseyevich Anan'yev, "Nauka", 4000 copies, 328 pages]

[Text] The book gives the basics of the theory of optical cavities, and examines the factors that determine divergence of laser emission. Major emphasis is given to the problem of producing narrowly directed radiation; various methods are outlined for reducing angular divergence. Considered in greatest detail are the properties of lasers with so-called unstable optical resonators. Methods of calculating and optimizing them are outlined, and the particulars of designs used in a variety of laser devices are discussed. The book also gives some information on factors giving rise to optical inhomogeneities in an active medium, the nature of such inhomogeneities, and methods by which their influence can be reduced. Figures 112, tables 3, references 343.

Introduction

Development of Concepts of the Optical Cavity as a Device for Producing Narrowly Directional Emission

The first papers on the feasibility of making resonators in the optical band for stimulated emission of coherent radiation were published by Prokhorov, and also by Shawlow and Townes in 1958. These papers to a great extent predetermined the course of research that led to the development of lasers.

As we know, laser action is based on the capacity of certain media under certain conditions to amplify luminous radiation passing through them. Therefore there is no doubt that a major role is played by the properties of the active medium itself and the method of stimulating it; however, the properties of the resonant cavity in which this medium is located also have an enormous influence on many characteristics of stimulated emission. Taking a central place among such characteristics is the angular divergence of emission. Here the resonator plays a truly decisive role: without a resonator, the active medium in itself as a rule

is capable of amplifying the radiation passing through it to equal advantage no matter what the direction of propagation.

Optical oscillators made their appearance much later than rf and microwave oscillators. Therefore the concepts and terminology borrowed from these related fields are extensively used in describing optical oscillators, and we will continue this practice.

To convert an oscillator to an amplifier, it is necessary in the language of electronics to close the output of the amplifier to its input, to set up a feedback circuit (Fig. 1, a). The essence of the feedback circuit is that part of the amplified radiation goes back into the system, is amplified again and so on, in this way maintaining a continuous signal--oscillation. Oscillators in the optical band amplify a light beam rather than an electric signal. In this connection, the feedback circuit must meet new requirements: after transmission through the feedback circuit the beam must retain its original direction of propagation and structure. The simplest analog of Fig. 1, a that meets these requirements is the optical resonance shown in Fig. 1, b. Actually, such resonators, called ring cavities, have found some application. However, the first resonator in optics was a conventional Fabry-Perot interferometer made up of two flat mirrors (Fig. 1, c). One mirror is partly transparent, and the stimulated emission is coupled out through it. The principal difference of this resonator from the ring cavity is that the feedback circuit passes through the same active medium, and the emission is repeatedly amplified.

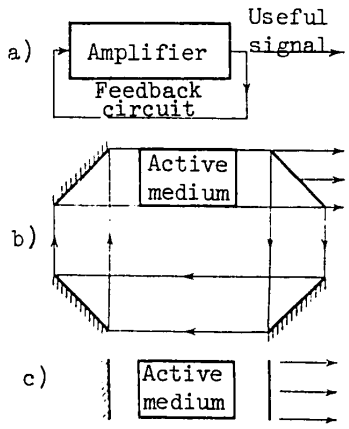

Fig. 1. Diagrams of oscillators: a) oscillator in electronics; b) oscillator in optics; c) laser with flat optical cavity

The Fabry-Perot interferometer has been such a successful resonator system that even today it is the most widely used type of laser cavity. Such popularity is due not only to extreme simplicity, but also to the capability of attaining high energy characteristics of output emission (the reasons for this will be taken up in section 1.4). However, the situation with regard to divergence of emission stimulated in flat-mirror cavities was trivial. The origin of comparatively large divergence is explained to a great extent by theoretical analysis of the properties of the flat optical cavity, which can be done by methods developed previously for resonant cavities in the microwave band. Such analysis shows that transmission through the feedback circuit in a flat cavity reproduces not just any beam directed along the axis and nearly parallel with it, but only a beam with strictly defined distribution of the amplitude and phase of the wave front. This beam is called the fundamental waveform (mode) of the cavity. What is more remarkable however, is that there are also beams (modes) that are reproduced with somewhat greater attenuation in which emission propagates at small but nonetheless noticeable angles to the axis of the cavity. These beams form a

discrete set; the angle of inclination to the axis for modes that are neighbors in classification differs by approximately half the diffraction angle.

Thus a flat cavity in some sense (and, of course, within certain limits) is indifferent to the direction of emission propagating through it. The roots of such indifference are in the fact that upon passage through the feedback circuit the oblique beams, like the axial beam, retain their original directions of propagation; they are prevented from "walking off" by edge diffraction. The mechanism of such diffraction will be taken up in section 2.2.

Because of differences in attenuation, the different off-axis modes have somewhat different thresholds of excitation; however, because of nonlinearity of the medium, these modes can be present simultaneously in the stimulated emission (Chapter 2), which should lead to a large angular divergence of the beam. For this reason, flat cavities with large aperture cannot give small beam divergence even when the medium is highly homogeneous.

Such is the situation in the idealized case of an optically homogeneous medium. An even greater disadvantage of the flat cavity from the standpoint of the directionality of radiation is the extremely sharp dependence of the field distribution in the cavity on slight distortions of shape (deformation). This can be explained by the simple example of a misaligned cavity. Nonparallelism of the mirrors is equivalent to insertion of an optical wedge in the feedback circuit that changes the beam direction by an angle δ that is twice the angle of misalignment. If we send a parallel beam into such a cavity, it will be turned through an angle δ after the first pass, through 2δ after the second and so on. Its displacement in the transverse direction will increase even faster, and a considerable part of the radiation will begin to leave the system, missing the mirrors. After a certain number of passes (a fairly large number for small δ), the beam shape is distorted so much that it becomes impossible to analyze the process of further propagation without consideration of diffraction effects. Therefore it is no simple matter to represent the steady-state field distribution in graphic form. In essence this distribution is the result of equilibrium between processes of diffraction and beam rotation. We emphasize that this equilibrium is reached after a process of accumulation of aberrations over a number of passes. It is also noteworthy, as shown by analysis (section 2.5), that there is a rapid rise in the number of passes over which aberrations accumulate with an increase in the cross sectional dimensions of the optical cavity. Therefore flat cavities with mirrors of large dimensions are particularly sensitive to slight aberrations.

The situation is similar, but even more complicated in the case of irregular deformations of the cavity. In general, the sources of such deformations are extremely varied: they include errors of manufacture and alignment of mirrors, initial optical inhomogeneity of the active medium, inhomogeneity induced during pumping due to nonuniform excitation and heating of the medium, scattering of light by microscopic inclusions, mechanical vibrations of the active element, turbulence of gas flow, and the list could be extended. It is no wonder that a great many papers have dealt with the problem of a nonideal flat resonator, most of them published in 1965-69. The results of research dealing with the most common principles of behavior of lasers with nonideal optical cavities will be given in section 2.5. Of course, noe of this research could eliminate the

fundamental flaws of the flat optical cavity, but it has been very useful for an understanding of the processes that take place in a real cavity.

In these same years, as much research was done to find some new solution of the laser beam divergence problem. Two areas of such research can be distinguished.

Representatives of one of these areas tried without giving up the flat cavity to put into the feedback circuit so-called angle correctors: filters that transmit radiation only in a narrow range of angles. Such filters can be made by different methods: on the basis of total internal reflection, by additional Fabry-Perot étalons, by a combination of lenses and irises. All these methods were tried; however, subsequently because of considerable complications and a number of fundamental difficulties that will be taken up in section 2.6, they found only a few special applications.

Proponents of the other area of research have attempted to solve the problem of divergence (or at least single-mode lasing) by altering the shape of the mirrors rather than by complications in the design of the optical cavity. In particular, there has been a thorough investigation of lasers with so-called stable resonators, in which one or both mirrors are slightly curved (the equivalent of placement of a weak positive lens in the feedback circuit). Obviously in such a system a steady-state beam with approximately uniformly distributed amplitude and phase and a front close to planar should have such a small cross section that the focusing effect of the mirrors is compensated by the defocusing of the beam due to diffraction. This is the source of the main disadvantage of stable resonators: they are capable of single-mode lasing only with very small volumes of the active medium. And it is in lasers with small volumes of the working medium that stable resonators are still being used; an example is the ordinary helium-neon laser. If the volume of the medium is large, wide beams are produced in stable resonators with a complicated beam structure corresponding to an angular divergence larger than in flat cavities under the same conditions (sections 2.3 and 2.4).

Some other forms of optical cavities with small diffraction losses have also been investigated (section 2.6), but these were also failures.

This situation led to the general opinion that the problem of directionality of radiation could not be solved by improving the optical cavity, and that the only possible way was to make multistage systems of a master laser and amplifiers (since amplifiers are not troubled with the effect of multiple accumulation of aberrations, like the flat cavity). A way out of this dilemma was suggested by Siegman's research with a simplified analysis of an "unstable" resonator (in the accepted classification; section 1.2), which is formed by two convex mirrors. This analysis showed that in such a resonator, just as in the ideal flat optical cavity, there is a solution in the geometric approximation, only diverging rather than parallel beams propagate in both directions along the cavity, and part of the radiation passes the mirrors (section 3.1). At first Siegman's paper did not stir up any particular interest: some researchers were already working with unstable resonators, and were getting only undesirable side effects rather than encouraging results (see the beginning of section 3.1). And Siegman himself even switched his attention to the unusual features of edge effects in unstable resonators, devoting some years to the study of this problem, which is interesting,

but as we will show below is far from decisive. From the standpoint of directionality of radiation, the most interesting peculiarities of unstable resonators were discovered only with analysis of the influence of aberrations on steady-state field distribution. It was as a result of such an analysis that it became clear that the resonator considered by Siegman was only the first of an extensive class of cavities in which feedback conforms to a totally new algorithm that has a number of fundamental advantages.

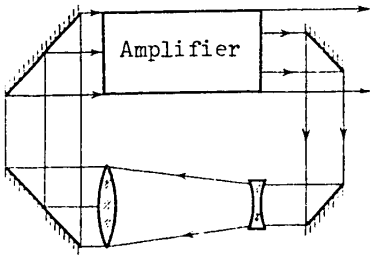

Fig. 2. Diagram of a laser with unstable resonator

The essence of this new algorithm is clarified by Fig. 2. In the flat cavity, part of the radiation from the entire cross section of the output beam was introduced into the feedback loop (see Fig. 1, b). In the unstable resonator as a rule all the radiation is fed back, but only from part of the cross section. For reproducibility of the process, the feedback circuit obviously has to be made in such a way that the beam is widened. In Fig. 2, the wave front is planar and the beam is expanded by a telescopic system, but quite different versions are possible. In particular, the dimensions of the cross section of a parallel beam are also altered when it is reflected from a diffraction grating, and when it passes obliquely through the interfaces of media with different indices of refraction. Thus lenses and spherical mirrors are not at all obligatory equipment for an unstable resonator.

Now let us examine what advantages could be realized by what would seem to be such a minor change in the algorithm. As in the case of a flat cavity, let an

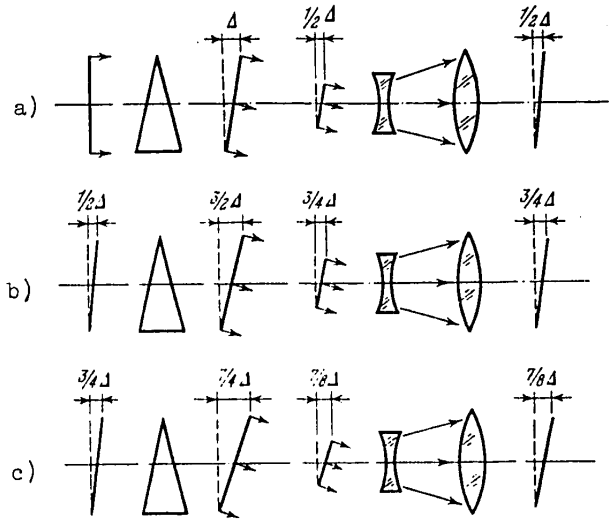

Fig. 3. Accumulation of wave aberrations in an unstable resonator when an optical wedge is inserted

optical wedge be inserted within the system, leading to rotation of the beam, and let this rotation correspond to a magnitude of wave aberrations Δ (Fig. 3, a). Part of the beam goes to the feedback loop; in the case shown in the figure, its transverse dimension is half the size of the entire beam. On this part of the cross section, the magnitude of the wave aberrations is of course equal to $\frac{1}{2}\Delta$. When the cross section of the beam is stretched out by the methods enumerated above, the magnitude of the wave aberrations does not change; therefore by the beginning of the next cycle a beam arrives at the input of the system with aberration of $\frac{1}{2}\Delta$, rather than Δ as in the case of a flat cavity. Upon passage through the system, another Δ is added (see Fig. 3, b) and by the end of the second cycle the magnitude of the wave aberrations becomes $\frac{3}{2}\Delta$. By the beginning of the third cycle it is $\frac{3}{4}\Delta$, by the end -- $\frac{7}{4}\Delta$ (Fig. 3, c) and so on. It can be seen that this quantity in the limit approaches 2Δ. Thus the wave aberrations in the steady state are found to be only twice the level in a single pass. In this situation, shifting of the beam in the transverse direction does not generally play any particular part: it leads only to slight redistribution of the fractions of the beam passing to different sides of the output mirror, but the feedback loop remains completely filled.

In the case of arbitrarily distributed sources of aberrations, of course there are changes in the quantitative factors, but the qualitative patterns remain the same: the accumulation of wave aberrations of the beam takes place over the calculated number of passes (see section 3.2). As the fraction of the beam cross section directed into the feedback loop decreases, this number approaches unity, a quantity typical of single-stage amplifiers.

We can also conclude from the example given in Fig. 3 that in the unstable resonator there is only one form of wave front that is retained after the beam passes through the feedback loop. Actually the direction of the light beam admitted to the optical cavity rapidly approaches the unique equilibrium direction (which in the case of Fig. 3 corresponds to steady-state wave aberrations 2Δ). Thus in contrast to the flat optical cavity, the unstable resonator displays rigorous selectivity with respect to the direction of emission; it would seem that here the effects of multimode lasing should have no influence on the magnitude of angular divergence.

These encouraging deliberations concerning the properties of unstable resonators, implied by the simplest geometric approximation, are confirmed as well by more thorough analysis in the diffraction approximation (section 3.3). Moreover, detailed acquaintance with the properties of unstable resonators allows us to formulate the following statement: if the operation of a laser in which a large volume of comparatively homogeneous active medium has been used is strongly influenced by diffraction, this means that errors have been made in its creation. At first glance this statement seems to be paradoxical: in all previously used optical cavities the beam structure has been determined in the final analysis by diffraction. However, this statement has a firm logical basis. The final goal is to produce a laser with minimum angular beam divergence; this goal is fully attainable in a homogeneous medium. Beams with minimum divergence are those for which the wave front is flat or spherical; it is well known that propagation of such beams to short distances is beautifully described by the geometric approximation, without resorting to the concept of diffraction.

This covers the conceptual aspect, and we turn now to practice.

The scheme with two convex mirrors considered in Siegman's first paper was never used in that form, remaining a favorite subject of research for theoreticians in virtue of its symmetry. But then, a number of specialized schemes enabling solution of some problems in laser technology by much simpler means than before became obsolete.

Among these problems, of course, is the very problem of constructing simple laser emitters with high efficiency and low angular divergence of radiation. In most cases of practical importance, the so-called telescopic cavity (section 4.1) is suitable for solving this problem, being an asymmetric confocal system made up of a convex and a concave mirror. In this system the path of the rays differs from that of Fig. 2 only in the spatial congruence of two oppositely directed beams, i. e. in the same way that the scheme of Fig. 1, c differs from that of Fig. 1, b. Also of interest is the ring version of the telescopic cavity, wherein conditions are readily brought about such that the radiation flux propagating along the ring to one side, without the use of nonreciprocal devices, should be many times greater than the flux following in the reverse direction (section 3.5).

There are a number of new possibilities associated with the idea of utilizing the particular role that is associated with the paraxial region in the unstable resonator. This idea is as follows. If we trace the path of the rays in an unstable resonator over several cycles, we can see that radiation "spreads out" over the entire cross section from a small area that is contiguous with the line that is the axis of the resonator. By introducing emission into the region with predetermined temporal and spectral characteristics, we can obviously accomplish effective control of the radiation of the entire laser. When the "seed" radiation is taken from an external source and coupled in through an aperture in the mirror on the axis of the optical cavity, our device becomes simply a multipass amplifier with very high gain (section 4.3). As the emission intensifies, the cross section of the beam expands, which facilitates attainment of the limiting possible energy characteristics. Control of radiation properties on the basis of this principle can also be realized by making single lasers that have the valuable property that the cross sections of the control elements that are used in them (shutters, spectral selectors) are many times less than the cross sections of the output apertures.

Some special problems can be successfully solved by a slight modification of the feedback algorithm. As an example, we can cite the problem of stabilizing the direction of radiation; this problem arises in the widely encountered case where there is an optical wedge inside the resonator with a size that changes during the lasing pulse (e. g. because of mechanical vibrations of the active element). To strongly attenuate the influence of the wedge, it is sufficient to construct a feedback loop such that the beam is reversed in addition to expansion of the cross section. If this change is made in the version shown in Fig. 3, by the beginning of the second cycle the magnitude of wave aberrations is equal to -0.5Δ, by the end of the cycle it is $-0.5\Delta + \Delta$; by the beginning of the third cycle it is -0.25Δ, and by the end it is $+0.75\Delta$ and so on. In the final analysis a front is set up at the output of the system with aberration of 0.67Δ, i. e. one-third of the value in the case of Fig. 3. Let us note that both Fig. 3 and

the example now being considered are essentially different types of telescopic ring cavities. In the case of non-ring systems where the beam in following the feedback loop passes through the same wedge, designs can be developed with even better stability of the direction of the output beam (section 3.5).

Finally, we must not fail to mention problems that arise with the appearance of a number of new types of lasers. For example in the so-called fast-flow lasers the active medium passes through the optical cavity in the transverse direction, often with excitation beforehand rather than in the cavity. This leads to radiation field distribution patterns that are totally different from those of previously existing lasers; in particular, when flat mirrors are used, lasing can be localized in a narrow zone close to the edge of the cavity where the active medium enters. The density of the stimulated emission there is naturally extremely high. A completely analogous situation occurs in transversely pumped Raman lasers. Difficulties of this kind are easily overcome by using unstable resonators: a kind of self-balanced mode arises, and the radiation flux is distributed more or less uniformly over the cross section of the cavity (section 4.2).

All these possibilities were quite quickly realized in specific devices (see Chapter 4). Thus within only a few years after the publication of the first report on experimental observation of angular selection in an unstable resonator it became completely clear that this was the optical cavity that is optimum for the most diverse forms of lasers with narrow-beam radiation.

All the aspects mentioned above, as well as some other facets of the problem of divergence will be dealt with more rigorously and consistently later. Before we go into this, let us note one interesting feature of the history of this problem. We have just spoken of the extent to which solution of the problem of divergence is obstructed by appreciable inhomogeneities of the active medium. The results of considerable research in the early sixties (section 2.3) showed that difficulties also pile up rapidly with increasing diameters of the lasing beams: the diffraction limit of divergence is difficult to attain only in the case where the diameter of the active element is large, and the limit is correspondingly small. If beam diameter is reduced (e. g. by irising the cavity) to a size of the order of 1 mm or smaller, beam divergence as a rule is the diffraction level even when no special steps are taken.

The first gas lasers, typified by the pre-eminent helium-neon laser, operated on an active medium confined in a rather slender discharge tube, and produced a light beam of small diameter. The mixture itself was quite rarefied, and a negligible amount of power (by present-day standards of laser technology) was expended on excitation; therefore the active medium was nearly ideally homogeneous. Due to this confluence of circumstances, the developers of gas lasers did not come up against the problem of divergence in earnest for many years. It might seem to the superficial observor that this problem is specific in general to solid-state lasers, and arose primarily because of the imperfectness of solid active media. However, in recent years the intense development of gas laser physics has led to new types of lasers such as chemical, gasdynamic and other types, with power many orders of magnitude greater than that of the familiar helium-neon lasers. The rise in radiation power is being achieved by an increase in the pressure of the working medium, the dimensions of the space that it

occupies, and specific energy inputs on excitation. All this entails considerable optical inhomogeneities of the medium. Thus the problem of beam divergence has turned out to be a problem of all lasers with high emission power, not just solid-state lasers. The developers of high-power gas lasers are now coming up against just about the same difficulties that had previously been encountered by those developing the solid-state laser, and they are using just about the same methods of solving them. For this reason, research in the field of gas lasers has not added much new information on methods of angle selection. Most of the research that has played a large part in solution of the problem of divergence, and that will be used in this book, has been on solid-state lasers.

Contents

6610
CSO: 1862/171

UDC 621.373.826.038.823

CW EMISSION OF AN IODINE PHOTODISSOCIATION LASER

Moscow KVANTOVAYA ELEKTRONIKA in Russian Vol 8, No 4(106), Apr 81 pp 830-837

[Article by V. Yu. Zalesskiy, L. S. Yershov, A. M. Kokushkin and S. S. Polikarpov]

[Text] An investigation is made of prolonged (83 s) lasing on a wavelength of 1315 nm upon illumination of gaseous iodotrifluoromethane flowing along a laser tube by using radiation from two low-pressure mercury vapor lamps. This required 6.5 liters of CF_3I at a pressure of 0.82 atm. It is shown that the results of experiment agree well with numerical calculation. The authors discuss the feasibility of achieving continuous emission of a photodissociation laser over a longer time period.

1. Introduction

A number of publications that have appeared in recent years show interest in continuous emission of an iodine laser on a wavelength of 1315 nm. The problem has been solved by two methods. One of these [Ref. 1-5] used the rapid collisional transfer of electron excitation from metastable molecules of oxygen $O_2(^1\Delta g)$ to iodine atoms. Lasing was observed for several minutes when metastable oxygen was produced chemically [Ref. 3-5]. An increase in lasing duration is apparently impeded by depletion of the reagents and/or accumulation of harmful reaction products.

The other method is photodissociation of molecules of the RI type, where R is a perfluoroalkyl. Continuous emission of an iodine photodissociation laser was first achieved in Ref. 6, and lasted about 1 s. Excited iodine atoms were produced upon photodissociation of molecules of the iodide $(CF_3)_3CI$ with radiation from two high-pressure mercury vapor lamps. Lasing duration was determined by the supply of working gas which flows along a laser tube with illuminated length of 17 cm at a velocity of ~30 m/s. Intentions to get continuous lasing by a similar method but with photodissociation of CF_3I molecules using low-pressure mercury vapor lamps have also been reported in a recently published paper [Ref. 7]. However, the estimates cited there of optimum velocity of the gas (8 m/s) with a laser tube 2 m long at a pressure of 20 mm Hg are wrong according to our calculations, and continuous lasing could scarcely be achieved under such conditions. At the same time, our own estimates show that the use of CF_3I for solving this problem is completely sound.

Even though the attainment of continuous emission of an iodine laser based on photodissociation of molecules may also involve the problem of irreversible consumption of the working gas, nevertheless in the given case this problem may be less severe in connection with the high efficiency of the process of inverse recombination:

$$R + I \xrightarrow{k_1} RI, \tag{1}$$

which is characteristic of the perfluoroalkyliodides.

In this paper we analyze conditions of getting cw action in an iodine photodissociation laser, and also discuss the results of experiments in which, as far as we know, continuous lasing (for a duration of up to 83 s) has first been obsaerved on CF_3I pumped by low-pressure mercury vapor lamps.

2. Conditions of Continuous Lasing

Photolysis of any batch of working gas under iodine photodissociation laser conditions cannot be continued indefinitely for a number of reasons. Among these are overheating and pyrolysis of molecules of the working gas:

$$RI \xrightarrow{k_2} R + I, \tag{2}$$

the presence of channels of "irreversible" recombination: the processes

$$2R \xrightarrow{k_3} R_2, \tag{3}$$

$$2I + M \xrightarrow{k_4} I_2 + M, \tag{4}$$

quenching in the process

$$I^* + RI \xrightarrow{k_5} I + RI, \tag{5}$$

and finally, an increase in quenching rate in the process

$$I^* + I_2 \xrightarrow{k_6} I + I_2 \tag{6}$$

in connection with the accumulation of the only strongly quenching product (in the unheated active medium), molecules of I_2. According to our calculations, in the case of CF_3I the optimum time Δt_{opt} for illumination of the working gas is determined by the last factor.

The conclusion extends to the region of optimum pressures (1-3 kPa) and to the pumping rate that is of practical interest. When CF_3I is pumped by radiation from low-pressure mercury vapor lamps, the characteristic probability γ of photodissociation of molecules lies in a range of 0.05-1.0 s^{-1}. It is important to note that this conclusion loses force in the case of pumping characteristic of pulsed iodine photodissociation lasers, where $\gamma \sim 10^2$-10^4 s^{-1}. (An analysis of computational and experimental data available to us on conditions of pulsed iodine photodissociation lasers will be published in a separate paper.) Let us also note that this conclusion remains in force for $R = C_2F_5$, $CF(CF_3)_2$ as well, but is not valid for example in the case of $C(CF_3)_3$.

In the latter case, Δt_{opt} is determined by process (5), i. e. quenching by molecules of the iodide $(CF_3)_3CI$ itself. By careful distillation and evacuation to 0.1 Pa in the case of this iodide we were able to determine $k_5 = (7 \pm 2) \cdot 10^{-16}$ cm^3/s from luminescence attenuation on 1315 nm, which is more than an order of magnitude greater than k_5 for CF_3I ($5.4 \cdot 10^{-17}$ cm^3/s [Ref. 8], $3.3 \cdot 10^{-17}$ cm^3/s [Ref. 9]) and appreciably worsens the outlook for using this iodide in a cw iodine photodissociation laser. Besides, on a wavelength of 254 nm (radiation of low-pressure mercury vapor lamps) the absorption cross section of $(CF_3)_3CI$ molecules ($1.3 \cdot 10^{-19}$ cm^2) is small compared with the value of $4.2 \cdot 10^{-19}$ for CF_3I. An advantage of using $(CF_3)_3CI$ is the inefficiency of recombination channel (3) [Ref. 10], which is important for making a cw iodine photodissociation laser with circulation of the working gas in a closed system.

The finiteness of Δt_{opt} leads to the necessity of circulating the working gas through the sections of the laser tube that are being subjected to pumping. The rate of flow corresponding to maximum gain G on length Δl of the illuminated section of the laser tube in the case of longitudinal gas flow was estimated by numerical calculations in accordance with the kinetic model of an iodine photodissociation laser proposed in Ref. 11, but with the more precise constants of Ref. 12, 13, and with consideration of diffusion of I* atoms to the wall [Ref. 8]. The quantity $\alpha(\Delta t) = \int_0^{\Delta t} N(t)\,dt$ was calculated, which is related to gain $G(\Delta l)$ by the expression

$$\ln G = \sigma \int_0^{\Delta l} N dl = \sigma v \int_0^{\Delta t} N dt = \sigma \Delta l \frac{\alpha(\Delta t)}{\Delta t}, \qquad (7)$$

where N is the population inversion of laser levels; σ is the amplification cross section; $v = \Delta l / \Delta t$ is gas velocity. The radial dependence of gas velocity can be disregarded even in the case of laminar flow (realized in the experiments) if we are interested only in amplification in the paraxial part of the laser tube.

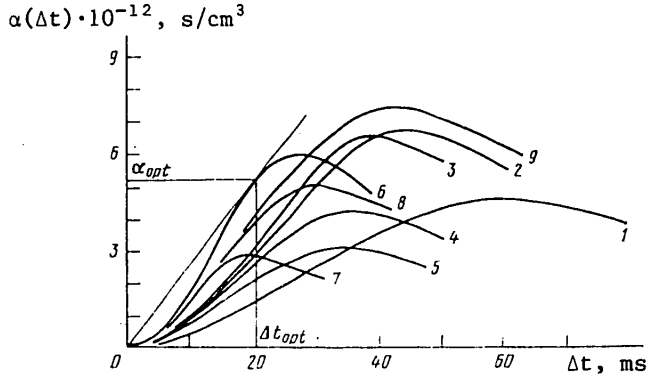

Fig. 1. Curves of $\alpha(\Delta t)$ in the case of CF_3I calculated for the conditions indicated in the table

Fig. 1 shows some results of calculations of the dependence $\alpha(\Delta t)$ for some values of pumping γ, concentration n and temperature T of CF_3I and the effective rate constant of quenching k_5 with consideration of possible contamination of CF_3I with quenchants.

TABLE

Curve # (Fig. 1)	$n \cdot 10^{-17}$, см$^{-3}$	$T^{1)}$, K	$\sigma \cdot 10^{18}$, см^2	γ, с$^{-1}$	$k_5^{2)} \cdot 10^{17}$, см^3/с	Δl_{opt}, см	$v_{opt}^{3)}$ м/с	$\alpha_{opt} \cdot 10^{-12}$, см^2/с	Gain$^{4)}$ дБ (%/pass)
1	2,5	300	5,6	0,05	11	41,0	2,94	3,6	0,21 (4,7)
2	»	»	»	0,10	»	34,0	3,53	5,8	0,40 (9,2)
3	5	»	4,3	0,05	5,5	32,0	3,76	5,9	0,33 (7,6)
4	»	»	»	»	11	26,5	4,53	3,6	0,24 (5,6)
5	»	»	»	»	16,5	24,0	5,00	2,5	0,19 (4,3)
6	»	»	»	0,10	11	20,0	6,00	4,9	0,44 (10,1)
7	10	»	2,9	0,05	»	15,5	7,75	2,5	0,194 (4,5)
8	»	400	2,5	»	»	22,0	5,47	4,1	0,194 (4,5)
9	»	500	2,2	»	»	26,0	4,63	5,3	0,187 (4,3)

Notes: 1) at $\gamma = 0.1$ s^{-1} the gas temperature was not determined by photochemistry, but rather by the heating of the laser tube walls by the pumping lamps to 200-300°C, depending on the conditions of air cooling; 2) the use of values of k_5 double ($11 \cdot 10^{-17}$ cm^3/s) and triple ($16.5 \cdot 10^{-17}$ cm^3/s) the value obtained in Ref. 8 reflects the intent to determine the influence of contamination of the working gas that may occur under the operating conditions of the iodine photodissociation laser; 3) the value of v_{opt} was calculated for $\Delta l = 12$ cm; 4) the gain was calculated for a laser tube (see Fig. 2) with consideration of the fact that radiation is amplified by a factor of G_{max} with 8 round trips of the optical cavity, i. e. in accordance with the formula $10 \lg (G_{max}^8) = 4.34 \cdot 8\sigma v_{opt} \alpha_{opt}$ [dB]; in parentheses: $100 \ln (G_{max}^8) = 100 \cdot 8\sigma v_{opt} \alpha_{opt}$ [%/pass] ($\sim 800 (G_{max} - 1)$).

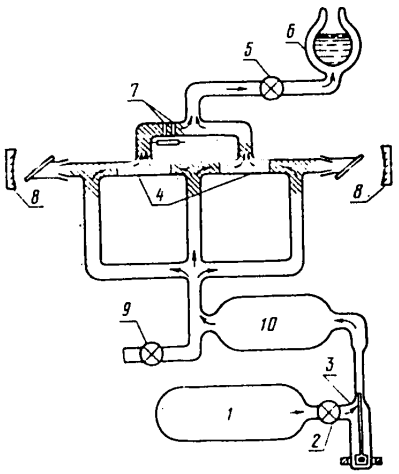

Fig. 2. Diagram of cw iodine photodissociation laser:

1--6.5-liter bottle of working gas; 2--valve; 3--inlet with permanent-magnet regulation of gas flow; 4--illuminated sections of the laser tube; 5--valve; 6--liquid nitrogen trap; 7--device for measuring the lifetime of iodine atoms and gas velocity; 8--resonator mirrors; 9--valve for connection to evacuation or inlet system; 10--3-liter buffer tank

The logarithm of the gain is proportional to $\alpha(\Delta t)/(\Delta t)$ (see (7)). Maximum gain G_{max} corresponds to points of tangency (Δt_{opt}, α_{opt}) of curves $\alpha(\Delta t)$ with straight lines passing through the coordinate origin. From this we can readily find $\ln G_{max} = \sigma \Delta l \alpha_{opt} / \Delta t_{opt}$ and $v_{opt} = \Delta l / \Delta t_{opt}$. The value of σ for the strongest hyperfine component of radiation on frequency ν_{34} ($F = 3$, $F' = 4$) was found from data of Ref. 14.

The table summarizes some results of calculations showing that gain sufficient for overcoming the lasing threshold may be attained at a low gas velocity obviously corresponding to laminar flow (Reynolds number on the order of 1000 or less) if a laser tube is used that consists of a number of relatively short illuminated sections (4 in Fig. 2) with $\Delta l \approx 10$-20 cm connected in parallel in the flow scheme.

3. Experiment

Continuous lasing on a wavelength of 1315 nm was observed with flow of gaseous CF_3I through a quartz tube with inside diameter of 16 mm placed between two cylindrical low-pressure mercury vapor lamps fed from a 50 Hz ac line. The lamps were developed by Yu. A. Martsinkovskiy and S. A. Yakovlev, and operate in modes close to those described in Ref. 15 if we disregard the fact that they were designed for supply from alternating current, as opposed to those of the Brown Boveri Company, and therefore they have two incandescent electrodes each. The length of the working section of the lamps is 80 cm, diameter 100 mm, working current 8 A, voltage 100 V, temperature of the mercury branch tube 50-70°C. A more detailed description of the design and an investigation of the characteristics of these lamps will be published in a separate article. The length of the illuminated part of the laser tube was 48 cm. The gas flow branched as shown in Fig. 2 into four parts flowing around the laser tube in a path with length of $\Delta l = 12$ cm at a velocity of 2.5 m/s. This velocity refers to the paraxial part of the laser tube, and in view of parabolic radial distribution is close to the maximum. The given value of the velocity was determined from the location of the delayed maximum on the oscillogram of attenuation of luminescence of $\lambda = 1315$ nm that was excited by an IFP-600 flash tube simultaneously in two cross sections of quartz tube 7 (Fig. 2) separated by a distance of 3 cm along the gas flow, and was recorded by a germanium photodiode close to the lower (downstream) cross section of this tube. Fig. 3 [photo not reproduced] shows one of the oscillograms corresponding to the conditions of the experiment. Diffusion of atoms of I* to the wall considerably weakens contributions to the luminescence signal on the part of the sections of gas flow near the wall.

The ends of the laser tube are fitted with quartz windows 2.8 mm thick set at the Brewster angle. Concave spherical mirrors (8 in Fig. 2) were used with radius of curvature of 1 m and transmission of 0.2% on a wavelength of 1315 nm. The length of the cavity was 140 cm. Gas flow arose due to the pressure differential between the gas stored in bottle 1 and the gas in liquid nitrogen trap 6 that acted as the receiver of the used working fluid. The velocity and pressure of the gas in the laser tube could be regulated by inlet 3 with magnetic flow regulation and by valve 5 preceding the trap. Lasing arose when valve 2 was opened after a reliminary 5-minute warmup of the mercury vapor lamps. At a pressure of the stored gas of 80 kPa (0.82 atm) the lasing duration reached 83 s (Fig. 4 [photo not reproduced]). During this time the gas pressure in the laser tube did not exceed 3 kPa. According to our estimates, pressure increases (due to buffer tank 10) for about 10 s, after which a slow decline sets in. Fig. 4 shows a recording of the signal of the germanium photodiode that registers the radiation passing through one of the mirrors. It can be clearly seen that in the vicinity of maximum pressure the laser emission power falls off ($t \approx 13$ s). At the 26-th second, the cavity close to the other mirror was covered for 3.3 s by a glass plate oriented approximately parallel to the plane of the Brewster window. As Fig. 4 shows, this resulted in almost total suppression of lasing. Lasing was cut off when the pressure of the

gas in bottle 1 fell to 15 kPa. In one of the experiments, stable cw lasing was observed at $\Delta l = 10$ cm.

Fig. 5 [photo not reproduced] shows oscillograms of the lasing (curve 1) and pumping (curve 2) signals. Pumping radiation on $\lambda = 254$ nm was recorded by "sun-blind" photocell F-7, and the laser emission was registered by a germanium photodiode. The mercury lamps were fed in phase, ensuring 100% modulation of UV radiation on a frequency of 100 Hz. The laser emission signal indicates a spiked mode of lasing. The time intervals of 1-2 ms when lasing is absent correlate with pumping. Lasing usually appears when pumping reaches a level of 50% of the maximum power. Laser resonator losses were estiamted in experiments with a xenon flash tube IFP-2000 placed close to the laser tube, from the change in delay of the beginning of lasing and emission power when a thin quartz plate was inserted in the cavity. According to these data, losses amounted to 3% per round trip. This shows that the unsaturated gain corresponds to 6% per pass in the maxima of pumping radiation.

The quantity γ was determined from the signal of photocell F-7 with known absolute sensitivity on the 254 nm line. For the conditions of our experiments it was 0.05 ± 0.02 s^{-1}. In doing this, the lamps were placed on opposite sides of the laser tube at a distance of 3 mm away, and the illuminator was practically unused. We can easily convince ourselves that the measured saturated gain is close to the calculated value (see the data of the table for experiments 1 and 4). We need only consider the reduction in v_{opt} with heating (see experiments 7-9) and the fact that the gas used was not entirely free of quenchants. This is shown by measurements of the lifetime of atoms of I* made to check the purity of the working gas by means of device 7 (see Fig. 2) from attenuation of luminescence on $\lambda = 1315$ nm. These measurements gave a value of the rate constant k_5 that was double the value obtained in Ref. 8. Under the conditions of the given laser system we rarely managed to purify the working gas to give values of k_5 close to those quoted in the literature [Ref. 8, 9], and it required a great deal of time.

4. Discussion of the Results

The data given above show that the duration of cw lasing on $\lambda = 1315$ nm that we observed in the mode of single passage of the working gas through the laser tube is approximately two orders of magnitude greater than the duration of continuous lasing observed in Ref. 6 on $(CF_3)_3CI$. This difference is partly due to the fact that the latter has a much lower saturated vapor pressure at room temperature than CF_3I. For an identical supply of both gases, $(CF_3)_3CI$ requires a much larger volume. For use as an intermediate quantum frequency standard [Ref. 16], the possible lasing duration must be much longer than that which we have achieved. The results described above confirm our estimates of the feasibility of achieving cw emission without replenishment of the working gas for a considerably longer time when cyclic circulation of the gas in a closed system is used with a cooler for removing the molecular iodine that is the only harmful photolysis product. These estimates show that under the conditions of experiment 4 (see the table) over an illumination time of 40 ms ($\sim\Delta t_{opt}$) in the absence of lasing the irreversible consumption of working gas is 0.065% (final products I_2 and C_2F_6), i. e. 33% of the degree of photodissociation $\gamma\Delta t = 0.2\%$.

In experiments without lasing for similar conditions, an amount of molecular iodine corresponding to an irreversible consumption of 0.088% was determined by distillation

and weighing. It can be expected [Ref. 17] that under conditions of laser emission the irreversible consumption will be considerably reduced. But even if this does not happen, the estimate od continuous lasing time Δt_c under conditions of cyclic circulation with the same amount of gas supply (43.5 g) and the same values of velocity and pressure in the laser pumping tube and Δl gives $\Delta t_c > 100$ minutes if we assume that the time of one cycle $\Delta t_1 = 1$ minute, and the number of cycles $m > 100$ corresponds to 10% irreversible consumption of working gas at a consumption of $<0.1\%$ in each cycle ($\Delta t_c = \Delta t_1 m$).

The accumulated products of molecule C_2F_6 show an extremely low rate constant of quenching ($8 \cdot 10^{-18}$ cm^3/s [Ref. 19]), and the vapor pressure of molecular iodine at the temperature of the cooler (-60°C)* is sufficiently low even without consideration of the reduction in k_6 due to heating of the laser tube (in our experiments it reached 300 K in steady-state operation of the mercury vapor lamps). The power of the laser emission passing through the mirror with transmission of 0.1-0.2% as measured by the IMO-2 instrument was 0.2 mW. Without any changes in the operating conditions of the mercury vapor lamps or the mode of gas circularion, this power can apparently be increased by 2-3 orders of magnitude. To do this, we must optimize the extraction of emission from the cavity, i. e. its useful losses, and use mirrors with radius of curvature of ~30 m to considerably increase the diameter of ihe lasing region, which under our conditions was 0.9-1.2 mm, i. e. 0.3-0.5% of the cross sectional area of the laser tube.

Knowing the degree of photodissociation of the working gas per cycle (0.2%) and the velocity of the gas in the laser tube (3 m/s) we can estimate the limiting power of a laser of the given design, which would be reached at a very low quenching contribution and rapid depopulation of the lower level in process (1). It is determined from the formula

$$W = \eta k s v n \gamma \Delta t h \nu f^*,$$

where η is the ratio of useful to total cavity losses, $k = 4$ is the number of branches of the gas flow, s is the cross sectional area of the lasing region (~1.5 cm^2), $h\nu$ is the energy of a photon on $\lambda = 1315$ nm ($1.5 \cdot 10^{-19}$ J), f^* is the quantum yield of atoms of I* (0.9). For $\eta = 0.7$, $v = 3$ m/s, $n = 5 \cdot 10^{17}$ cm^{-3}, $\gamma = 0.05$ s^{-1} and $\Delta t = 40$ ms, we get $W = 0.17$ W. The power can be further increased by increasing the efficiency of utilizing pumping (the illuminator), the number and cross section of the channels (branches of the gas flow) and accordingly (under conditions of cyclic circulation) the productivity of the device that puts the gas into motion and of the cooler.

In conclusion we consider it our pleasant duty to thank Ye. B. Aleksandrov, who stimulated our interest in achieving cw emission of photodissociation lasers, and also S. A. Yakovlev and Yu. A. Martsinkovskiy for developing the low-pressure mercury vapor lamps, and V. I. Smirnova, V. G. Borodenetskiy, N. F. Prokhorov and B. S. Baranov for making these tubes.

---

*Such a method of removing I_2 is not suitable for $(CF_3)_3CI$ in view of the fact that the vapor pressure of this iodide is too low at t = -60°C.

REFERENCES

1. Derwent, R. G., Thrush, B. A., CHEM. PHYS. LETTS, Vol 10, 1971, p 591.

2. Pirkle, N. J., Wiesenfeld, J. R., Davis, Ch. C., Wolga, G. J., McFarline, R. A., IEEE J, QE-11, 1975, p 834.

3. Benard, D. J., McDermott, W. E., Bousek, R. K., Pchelkin, N. R., J. OPT. SOC. AMER., Vol 68, 1978, p 652.

4. Benard, D. J., McDermott, W. E., Pchelkin, N. B. et al., APPL. PHYS. LETTS, Vol 34, 1979, p 40.

5. Richardson, R. J., Wiswall, C. E., APPL. PHYS. LETTS, Vol 35, 1979, p 138.

6. Andreyeva, T. L., Virich, G. N., Sobel'man, I. I., Sorokin, V. N., Struk, I. I., KVANTOVAYA ELEKTRONIKA, Vol 4, 1977, p 2150.

7. Witte, K. J., Burkhard, K., Lüthi, H. R., OPTICS COMMUNS, Vol 28, 1979, p 202.

8. Zalesskiy, V. Yu., Krupeninkova, T. I., OPTIKA I SPEKTROSKOPIYA, Vol 30, 1971, p 813.

9. Dobychin, S. L., Mikheyev, L. D., Pavlov, A. B., Fokanov, V. P., Khodarkovskiy, M. A., KVANTOVAYA ELEKTRONIKA, Vol 5 1971, p 2461.

10. Yershov, L. S., Zalesskiy, V. Yu., Sokolov, V. N., KVANTOVAYA ELEKTRONIKA, Vol 5, 1978, p 863.

11. Zalesskiy, V. Yu., ZHURNAL EKSPERIMENTAL'NOY I TEORETICHESKOY FIZIKI, Vol 61, 1971, p 892.

12. Vinokurov, G. N., Zalesskiy, V. Yu., KVANTOVAYA ELEKTRONIKA, Vol 5, 1978, p 2112.

13. Vinokurov, G. N., Zalesskiy, V. Yu., Krepostnov, P. F., KVANTOVAYA ELEKTRONIKA, Vol 7, 1980, p 1770.

14. Zalesskiy, V. Yu., Polikarpov, S. S., KVANTOVAYA ELEKTRONIKA, Vol 2, 1975, p 1543.

15. Brändli, G., BROWN BOVERI MITT, Vol 62, 1975, p 202.

16. Orayevskiy, A. N., KVANTOVAYA ELEKTRONIKA, Vol 5, 1978, p 1850.

17. Andreyeva, T. L., Kuznetsova, S. V., Maslov, A. I., Sobel'man, I. I., Sorokin, V. N., PIS'MA V ZHURNAL EKSPERIMENTAL'NOY I TEORETICHESKOY FIZIKI, Vol 13, 1971, p 631; KHIMIYA VYSOKIKH ENERGIY, Vol 6, 1972, p 418.

6610
CSO: 1862/189

UDC 621.378.325

INVESTIGATION OF THERMAL SELF-STRESS OF A LIGHT PULSE IN A TURBULENT MEDIUM BY A METHOD OF STATISTICAL TESTS

Moscow KVANTOVAYA ELEKTRONIKA in Russian Vol 8, No 4(106), Apr 81 pp 873-877

[Article by V. P. Kandidov and V. I. Ledenev, Moscow State University imeni M. V. Lomonosov]

[Text] A Monte Carlo method is used to study propagation of a light beam in a randomly inhomogeneous medium under conditions of thermal blooming in the pulsed emission mode. The medium is broken down into layers, each of which is represented by a phase screen, a thin heat lens and a free diffraction section. The time change in statistical characteristics is determined from the set of solutions of the dynamic problem of passage of the beam through such a sequence of layers.

Propagation of beams of coherent emission in real media is accompanied by amplitude-phase distortions caused by inhomogeneity of the index of refraction and the influence of nonlinear effects. For some media (optical glasses, the atmosphere), it can be assumed that there exists a random field of permittivity $\tilde{\varepsilon}$ that originates independently of the nonuniformity of heat release upon absorption of radiation. In this case the light field intensity fluctuations that generate $\tilde{\varepsilon}$ lead to a fluctuating component of temperature T of the medium that causes irregular thermal refraction, and hence to random distortions of the phase and amplitude of the radiation. Thus the inhomogeneities of permittivity $\tilde{\varepsilon}$ are a random external factor for the closed nonlinear system formed by the beam and the medium.

The analytical study of nonlinear effects in propagation of radiation in randomly inhomogeneous media involves considerable difficulties. In Ref. 1 an equation was derived for the second-order coherence function assuming smallness of random deviations of temperature induced by the fluctuating intensity of the radiation. The time change in the spectrum of weak fluctuations of intensity for the light field of a plane wave in the pulsed emission mode was analyzed in Ref. 2 by the method of smooth perturbations.

In our paper we study the influence that thermal blooming has on the statistical characteristics of a light beam in the pulsed radiation mode. An examination is made of the behavior of the mean intensity profile, the dispersion profile and the coefficient of spatial correlation of intensity fluctuations. It is shown that fluctuations at first abate, and then tend to increase with increasing nonlinear refraction.

1. Consider propagation of a pulse with duration τ that meets the conditions

$$a/c_s \ll \tau < l_\varepsilon^2/4\chi,\ \tau_\varepsilon, \tag{1}$$

where a is the radius of the beam, c_S, χ are the speed of sound and thermal diffusivity in the medium, l_ε, τ_ε are the internal scale and "lifetime" of inhomogeneities of permittivity $\tilde{\varepsilon}$. In this case, for processes with time scale $t > a/c$ the isobaric approximation is valid in defining perturbations $\delta\varepsilon$ initiated by the beam: $\delta\varepsilon = (\partial\varepsilon/\partial T)T$. At the same time, it is assumed that the pulse is fairly short, and that thermal conductivity of the medium can be disregarded. Finally, the random field of $\tilde{\varepsilon}$ is considered "frozen" for the duration of the pulse. Under conditions (1), propagation of the beam along the OZ axis is described by the system of equations

$$2ik\frac{\partial E}{\partial z} = \Delta_\perp E + k^2\tilde{\varepsilon}E + k^2\frac{\partial\varepsilon}{\partial T}TE, \qquad \frac{\partial T}{\partial t} = \frac{\alpha nc}{8\pi\rho c_p}|E|^2, \tag{2}$$

where $\Delta_\perp = \partial^2/\partial x^2 + \partial^2/\partial y^2$; $t \in [0;\ \tau]$; $z \in [0,\ z_N]$; α, ρ, c_p, n are the coefficient of absorption, density, specific heat and index of refraction of the medium respectively.

In solving nonlinear nonstationary problem (2), the medium is broken down into layers $z_n - z_{n-1} = \Delta z$, $n = 1, \ldots, N$ each of which is represented by a sequence of a phase screen, a thin heat lens and a free diffraction section. In accordance with this, system (2) is replaced on each segment $[z_{n-1},\ z_n]$ by a network of the following equations:

$$2ik\frac{\partial E_e}{\partial z} = k^2\tilde{\varepsilon}E_e \quad \text{for } E_e(z_{n-1}) = E(z_{n-1}), \tag{3a}$$

$$\begin{cases} 2ik\dfrac{\partial E_T}{\partial z} = k^2\dfrac{\partial\varepsilon}{\partial T}TE_T \quad \text{for } E_T(z_{n-1}) = E_e(z_n); \\ T = \dfrac{\alpha}{\rho c_p}\displaystyle\int W_{n-1}dt, \text{ where } W_{n-1} = \dfrac{nc}{8\pi}|E(z_{n-1})|^2, \end{cases} \tag{3b}$$

$$2ik\frac{\partial E}{\partial z} = \Delta_\perp E \quad \text{for } E(z_{n-1}) = E_T(z_n), \tag{3c}$$

Such a representation is permissible if the diffraction effects can be disregarded on step Δz in determining the phase distortions due to nonlinearity and inhomogeneity of the medium, and if besides this step is shorter than the focal length of an individual random lens associated with the inhomogeneity of $\tilde{\varepsilon}$:

$$\Delta z < \min\left[\pi ka^2/(h\nabla_\perp R),\ kl_\varepsilon^2,\ l_\varepsilon/\tilde{\varepsilon}\right], \tag{4}$$

where h is the step of the space grid in plane z =const, $R(x,y,z,t) = k^2a^2\varepsilon_0^{-1}|\partial\varepsilon/\partial T|T$ (x,y,z,t) is a function that characterizes the phase lead in thermal self-stress $(\partial\varepsilon/\partial T) < 0$).

According to equation (3a) the complex amplitude of the electric field after passage through the phase screen takes the form

$$E_e(x, y, z_n) = E(x, y, z_{n-1})\exp(-iS_n),$$

$$S_n(xy) = \frac{k}{2}\int_{z_{n-1}}^{z_n}\tilde{\varepsilon}(x, y, z)\,dz. \tag{5}$$

If the correlation radius of fluctuations in permittivity is much shorter than Δz, then fields S_n have a normal distribution law and are statistically independent for different screens. Random fields S_n are formed on a two-dimensional grid with the aid of an algorithm of sliding summation [Ref. 3]. The least scale l_ε of inhomogeneities of field S_n has the order of the spatial step h of this grid.

The change in complex amplitude of the electric field with thermal phase advance is expressed in a form analogous to (5). Linear diffraction problem (3c) on segment Δz is solved by using the fast Fourier transformation algorithm with conversion to the Fourier transform and back to the function $E(x,y,z_n)$. In processing the results of a numerical experiment, averaging was used over 10-20 statistically independent realizations of the process of propagation. Additional averaging with respect to the angular coordinate in plane z = const is possible for axisymmetric beams.

2. Let random field $\tilde{\varepsilon}$ be homogeneous and isotropic. In this case the variance σ_S^2 of phase fluctuations on a screen does not depend on n. For spectral density $\Phi_\varepsilon(\kappa)$ corresponding to the Kármán model for atmospheric turbulence [Ref. 4]:

$$\Phi_\varepsilon(\varkappa) = 0{,}033 C_\varepsilon^2 (\varkappa_0^2 + \varkappa^2)^{-11/6}$$

($\kappa_0 = 2\pi/L_0$; L_0 is the external scale of turbulence), the variance takes the form

$$\sigma_S^2 = 0{,}195\, C_\varepsilon^2 \varkappa_0^{-5/3} k^2 \Delta z.$$

Let us consider the behavior of the statistical characteristics of a collimated beam of gaussian profile with propagation of a square pulse:

$$E(x, y, 0, t) = E_0(t) \exp(-(x^2+y^2)/2a_0^2),$$

$$E_0(t) = \begin{cases} 1, & t \in [0, \tau], \\ 0, & t \in [0, \tau]. \end{cases}$$

The length of propagation $z_N = 0.5\ ka_0^2$. On a gird with step $h = a/4$, condition (4) for inhomogeneities of the medium is satisfied for number of screens $N \geqslant 16$.

Following Ref. 4, we will characterize the influence of permittivity fluctuations as the beam propagates by the magnitude of the structure function of phase fluctuations of a spherical wave on the transmitting aperture $D_S(2a)$. For a network of N phase screens this function is defined by the expression $D_S(2a) = 4.46\sigma_S^2 \cdot N(a\kappa_0)^{5/3}$. The change in the quantity $D_S(2a)$ for N = 16 is achieved by using different σ_S^2 in producing a set of realizations. Nonlinear refraction of the beam is determined by the parameter of nonlinearity with instantaneous value of

$$R_0(t) = R(0, 0, 0, t) = \frac{k^2 a^2}{\rho c_p n} \left| \frac{\partial \varepsilon}{\partial T} \right| \alpha \int W_0 dt.$$

3. During propagation, the beam profile at the beginning of the pulse ($R_0 = 0$) spreads only as a result of diffraction and inhomogeneity of the medium (Fig. 1a). With time, a temperature field arises with an average component that causes thermal blooming. At $R_0 = 12$ an aberration ring begins to form that expands with time and has an intensity appreciably greater than the power density on the axis. This process at $R_0 > 10$ predominates over the beam broadening due to fluctuations of $\tilde{\varepsilon}$, and their influence is negligible for $D_S(2a) \leqslant 2.5$. During propagation in a randomly inhomogeneous medium the variance of the intensity fluctuations increases toward the periphery of the beam.

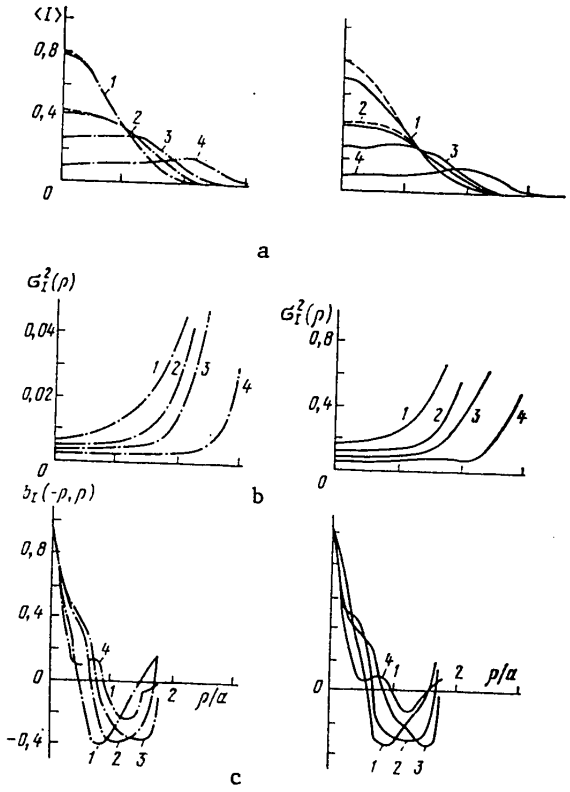

Fig. 1. Behavior of profiles of average intensity <I> (a), variance of intensity fluctuations $\sigma^2{}_I(\rho)$ (b) and coefficient of spatial correlation of intensity fluctuations $b_I(\rho)$ (c) of a light beam in plane $z = 0.5\ ka^2$ with increasing parameter of nonlinearity $R_0(t) = 0$ (*1*), 6 (*2*), 12 (*3*) and 36 (*4*); $D_S(2a) = 0$ (---), 0.1 (-•••-) and 2.44 (——)

Under conditions of thermal blooming, this increase slows down with time, and the dispersion profile $\sigma_I^2(\rho)$ becomes flat in the paraxial region (Fig. 1b). The dimensions of the flat part of the profile $\sigma_I^2(\rho)$ and of the beam region with relatively small change in <I>(ρ) coincide. Such behavior of the profile $\sigma_I^2(\rho)$ can be attributed to the change in time of the transverse distribution of intensity <I> in the nonlinear medium.

In the linear case for media with a low level of inhomogeneities $\tilde{\varepsilon}(D_S(2a) < 50)$ the abatement of the coefficient of spatial correlation of intensity $b_I(\rho)$ is characterized by a scale ρ_1 such that $b_I(\rho_1) = 0.5$. The region of negative correlations is due to wandering of the beam as a whole [Ref. 4]. In a nonlinear medium, scale ρ_1 increases with time due to thermal blooming on small-scale inhomogeneities of intensity (Fig. 1c). At the same time, due to the increase in the transverse size of the beam during thermal blooming, the region of negative correlations shifts toward larger radii. Further on ($R_0(t) \sim 30$), the appearance of the function $b_I(\rho)$ undergoes a qualitative change, scale ρ_1 decreases sharply. This can be attributed

to the fact that the light field in the paraxial region of the beam is close to a spherical wave, which is what determines the new scale of change in the correlation coefficient. In this connection, the boundary of the region of negative correlations, which is associated with the transverse size of the beam, shifts as before to larger radii ρ.

The fluctuations of intensity on the beam axis under conditions of thermal self-stress at first die down, and then show a tendency to increase (Fig. 2). The abatement of fluctuations is explained by the integrated nature of the thermal self-stressing effect, in which nonlinear refraction on intensity perturbations increases

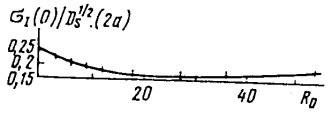

Fig. 2. Intensity fluctuations on the beam axis $\sigma_I(0)$ as a function of nonlinearity parameter $R_0(t)$; $z = 0.5\ k\alpha^2$

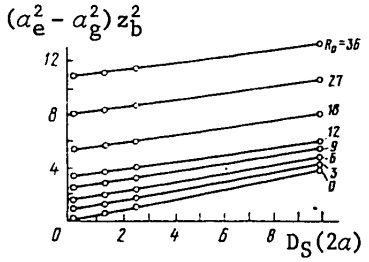

Fig. 3. Behavior of effective width a_e^2 of the beam as a function of $D_S(2a)$ and $R_0(t)$; $a_g^2 = a^2 + z^2/(ka)^2$; $z_b^2 = z^2/(ka)^2$

with time, reducing the fluctuations of I at $\partial\varepsilon/\partial T < 0$, which cause temperature inhomogeneities. The possibility of an increase of intensity fluctuations in thermal self-stress is explained in Ref. 2 by space-time modulation of intensity. It was estimated there that the increase in fluctuations begins at a value of the nonlinearity parameter (introduced in Ref. 2) of $\xi > 3.5$. For the given problem, we have $\xi_0 = \pi\sqrt{2}\,(z/ka^2)(a/h)\,R_0^{1/2}$ and a tendency toward an increase in fluctuations is observed only at $\xi_0 > 30$.

At the given values of $D_S(2a)$, turbulence and nonlinearity make an approximately additive contribution to the increase in the effective width of the beam (Fig. 3) [Ref. 5]. The increase in $D_S(2a)$ during propagation reduces the influence that thermal self-stress has on broadening.

4. In a stationary randomly inhomogeneous medium, radiation intensity fluctuations at the beginning of a pulse fall off due to thermal self-refraction on perturbations of the light field, and then begin to rise with increasing density of the absorbed energy. The characteristic scales of the profiles of statistical characteristics (average intensity $\langle I(\rho)\rangle$, variance of intensity fluctuations $\sigma_I^2(\rho)$, correlation coefficient of intensity fluctuations $b_I(\rho)$), and in particular the boundary of the region of negative correlation, are determined by the transverse size of the beam, which increases under conditions of thermal blooming. With time, as the density of absorbed radiation increases, a smaller scale of the correlation coefficient shows up that is close in magnitude to the case of a spherical wave.

REFERENCES

1. Vorob'yev, V. V., Shemetov, V. V., KVANTOVAYA ELEKTRONIKA, Vol 2, 1975, p 1428.

2. Agrovskiy, B. S., Vorob'yev, V. V., Gurvich, A. S., Pokasov, V. V., Ushakov, A. N., KVANTOVAYA ELEKTRONIKA, Vol 7, 1980, p 545.

3. Bykov, V. V., "Tsifrovoye modelirovaniye v statisticheskoy radiotekhnike" [Digital Modeling in Statistical Electronics], Moscow, Sovetskoye radio, 1971.

4. Gurvich, A. S., Kon, A. I., Mironov, V. L., Khelevtsov, S. S., "Lazernoye izlucheniye v turbulentnoy atmosfere" [Laser Radiation in a Turbulent Atmosphere], Moscow, Nauka, 1976.

5. Rohde, R. S., Buser, R. G., APPL. OPTICS, Vol 18, 1979, p 698.

6610
CSO: 1862/189

UDC 621.373.826.038.823

ELECTRIC-DISCHARGE CHEMICAL HF-LASER WITH HIGH PULSE RECURRENCE RATE

Moscow KVANTOVAYA ELEKTRONIKA in Russian Vol 8, No 4(106), Apr 81 pp 907-909

[Article by S. F. Zhuravlev, V. G. Karel'skiy, Yu. I. Kozlov, V. K. Orlov, A. K. Piskunov, Yu. V. Romanenko and Yu. I. Shcherbakov]

[Text] Stimulated emission is produced in an atmospheric-pressure HF laser on the chain reaction $H_2 + F_2$ initiated in a stream of the reactants by a volumetric transverse electric discharge with ultraviolet pre-ionization by a spark source of radiation. A pulse recurrence rate of 1 kHz is attained with lasing energy of 9 mJ in a pulse.

An investigation was made in Ref. 1 of the feasibility of making an atmospheric-pressure chemical laser based on a chain reaction of fluorine with hydrogen when mixtures are pumped through the laser cell that are resistant to the onset of detonation in the case of intense initiation. The working mixture in these experiments was prepared by diffusion mixing of premixtures containing fluorine and hydrogen in the flow, and the chemical reaction was initiated by ultraviolet radiation of flash tubes operating with a flash recurrence rate of 10 Hz.

This paper gives the results of an experimental study of a chemical HF-laser with high recurrence rate of emission pulses when the chain reaction is initiated by a volumetric transverse electric discharge.

Fig. 1 shows a diagram of the discharge chamber with the electric power supply for the volumetric discharge and the working mixture supply. Discharge chamber 1 was made of Teflon. Flat copper electrodes 2 measuring 6 x 2 cm with edges rounded along the perimeter were placed in the upper and lower walls of the chamber. The distance between the electrodes was 1.7 cm. Laser emission was coupled out through openings measuring 2 x 2 cm in the side walls of the chamber.

The discharge chamber was connected through gas line 3 to mixer unit 4 and the inlet system. On the other side, chamber 1 passed into an exhaust tube opening into a ventilated box equipped with a degasification system.

Premixes containing components of the working mixture diluted with helium were prepared in steel bottles before each startup of the facility. The oxidant premix contained fluorine and oxygen, and the fuel premix contained hydrogen. The premixes

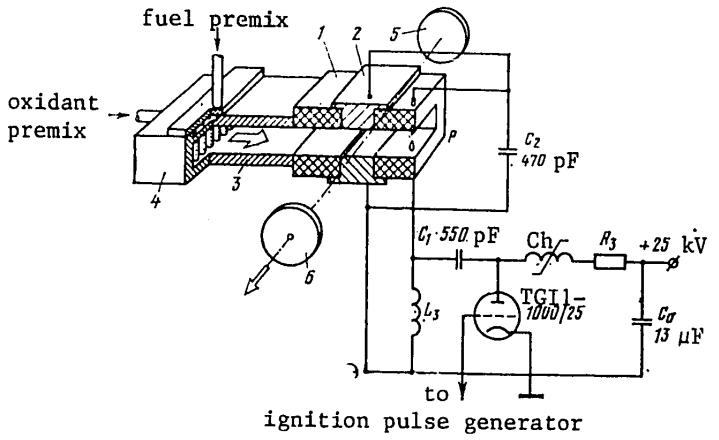

Fig. 1. Diagram of laser facility with the high-voltage circuit of the initiation system

entered the mixer unit 4 through high-speed pneumatic valves, and there the fuel premix was injected into the accompanying flow of oxidant premix through orifices 0.4 mm in diameter in the supercritical discharge mode. To intensify mixing, copper screens with a mesh of ~0.5 mm were installed across the gas line. The velocity of the gas stream was regulated over a range of 40-200 m/s by calibrated washers installed in front of the mixer unit and by the pressure in the bottles. There was no more than a 10% drop in the flowrate of the gases during a single run. The duration of intermixing of the premixes in the stream varied from 2 to 10 ms depending on the velocity of the flow.

To initiate the chemical reaction, an electric discharge was used with ultraviolet pre-ionization of the discharge gap analogous to Ref. 2. Ceramic capacitor C_1 with capacitance of 550 pF was charged from large electr[olyt]ic capacitor C_0 to a potential of 25 kV through inductance L_3, nonlinear choke Ch and resistor R_3. The nonlinear choke with magnetizing winding (not shown in the diagram) was designed and made by techniques presented in Ref. 3. Capacitor C_2 was made up of two ceramic capacitors of 235 pF each connected in parallel to the electrode by wide copper busbars. The gap P was formed by a 2 mm clearance between aluminum electrodes 4 mm in diameter located 7 cm away from the main electrodes downstream. During a single run at a pulse recurrence rate of 1 kHz the voltage across capacitor C_0 fell by 0.5 kV.

The laser cavity consisted of two copper mirrors. Opaque mirror 5 had a radius of curvature of 5 m, and flat mirror 6 had a 2 mm aperture for coupling out the radiation. The base of the cavity was 1.5 m.

The measurements of stimulated emission were made in the following arrangement. Unfocused laser radiation passed through a CaF_2 plate turned through an angle of 45° to the optical axis, and was incident on an IKT-1M calorimeter. Radiation reflected from the plate was incident through an attenuator on a Ge:Au photoresistor

cooled by liquid nitrogen. The shape of the lasing pulse registered by the photoresistor was recorded by an S8-7A oscilloscope; the voltage across the electrodes and the discharge current were registered by an ohmic divider and a resistor of 0.28 Ω respectively, and were fed to an S7-10B oscilloscope.

The facility operated as follows. The premixes entered the nozzle unit through the pneumatic valves, then went through the gas line to the discharge chamber and thence to the degasification system. Immediately after operation of the valves, the ignition pulse generator fed trigger pulses for 0.2 s to the grid of the thyratron with the necessary recurrence rate. Simultaneously with completion of operation of the ignition pulse generator a signal closed the pneumatic valves. Activation of the thyratron started resonant charging of capacitor C_2 from capacitor C_1 through gap P. The ultraviolet emission of gap P produced uniform ionization of the main discharge gap, and in the process of charging capacitor C_2 a high-voltage discharge was initiated in the gap, starting the chemical reaction in the working mixture.

Experiments were done on a mixture of composition $F_2:H_2:O_2:He = 2:2:0.2:95.8$ at an overall pressure of 0.1 MPa in the lasing zone. The composition of the working mixture was determined from the ratio of flowrates of the oxidant premix and fuel premix with accuracy of ±20%. The purity of the gases used was not checked.

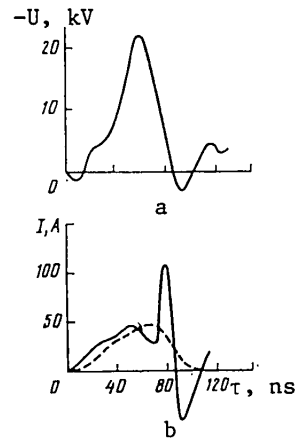

Fig. 2. Oscillograms of the voltage (a) and current pulses (b)

The solid curves on Fig. 2 show oscillograms of the voltage pulse across the discharge chamber and the current pulse of the volumetric discharge, which are the superposition of a set of practically identical single pulses with duration of ~80 ns (at the base) and recurrence rate of 1 kHz. As we can see from Fig. 2, within ~70 ns after the beginning of the high-voltage discharge, a breakdown of the main discharge gap occurred in each pulse, and the energy investment in the discharge was cut off in this pulse. At a pulse recurrence rate of 20-200 Hz the current pulse (broken curve in Fig. 2) started later and breakdown of the main discharge gap did not take place. The change in the discharge conditions (onset of breakdown) with an increase in the pulse recurrence rate to 1 kHz was caused by an increase in brightness of the luminescence of gap P due to heating of the spark electrodes [Ref. 4]. Reliable measurement of the energy E_{inv} invested in the discharge was unsuccessful since the current and voltage were measured in different experiments. According to preliminary estimates at a recurrence rate of the initiating pulses of 200 Hz, $E_{inv} \sim 30$ mJ.

Fig. 3 [photo not reproduced] shows the typical shape of a lasing pulse. The lasing pulse duration was 12.5 μs at the base and did not depend on the velocity of the flow or the pulse recurrence rate at fixed initiation energy.

At an initiating pulse recurrence rate of 20 Hz, the lasing energy in a pulse was 12 mJ. As the recurrence rate increased, a slight drop in lasing energy was

observed (down to 9 mJ in a pulse at a pulse recurrence rate of 1 kHz); apparently this effect is caused by a reduction in the energy contributed to the discharge. The average lasing power in this series of experiments did not exceed 10 W.

Our research has demonstrated the feasibility of making an atmospheric-pressure HF-laser with high pulse recurrence rate. In future research we will optimize the output characteristics of the laser.

In conclusion the authors thank Yu. L. Moskvin, Yu. A. Zav'yalov and F. F. Datchenko for cooperation in the work.

REFERENCES

1. Chen, H. L., Daugherty, J. D.. Fyfe, W., IEEE J., QE-11, 1975, p 648.

2. Baranov, V. Yu., Borisov, V. M., Kiryukhin, Yu. V., Kochetov, N. V., Pegov, V. G., Stepanov, Yu. Yu., KVANTOVAYA ELEKTRONIKA, Vol 5, 1978, p 1141.

3. Vdovin, S. S., "Proyektirovaniye impul'snykh transformatorov" [Designing Pulse Transformers], Leningrad, Energiya, 1971.

4. Marshak, I. S., ed., "Impul'snyye istochniki sveta" [Pulsed Light Sources], Moscow, Energiya, 1978.

6610
CSO: 1862/189

OPTICS AND SPECTROSCOPY

APPLIED PHYSICAL OPTICS

Moscow TRUDY MOSKOVSKOGO ORDENA LENINA ENERGETICHESKOGO INSTITUTA: PRIKLADNAYA FIZICHESKAYA OPTIKA in Russian No 450, 1980 (signed to press 31 Mar 80) pp 2, 83-87

[Annotation and abstracts of papers from book "Proceedings of the Moscow 'Order of Lenin' Power Engineering Institute: Applied Physical Optics", edited by Doctor of Physical and Mathematical Sciences, Professor V. A. Fabrikant, Moskovskiy energeticheskiy institut, 400 copies, 87 pages]

[Text] The experimental and theoretical papers included in this collection are unified by the common research topic of optical phenomena in resonators, gases and solids. The group of experimental papers deals with investigation of the characteristics of silicon emission power sensors, the coefficient of refraction and other properties of insulating films of MDS structures. Results are given from investigation of the interaction of electron beams with atoms and methods of calibrating excitation cross sections.

An important place among the theoretical papers is given to investigation of the statistical properties of reflected emission, analysis of the adiabatic hypothesis in quantum field theory, investigation of radiation processes in plasma in the presence of boundaries, statistical and polarization properties of bremsstrahlung, nonlinear processes in the continuous spectrum. In the papers devoted to the theory and methods of calculating optical cavities, a method of complex gaussian beams is proposed, and the method of beam matrices is generalized to arbitrary optical systems with smooth interfaces.

The collection may be of use to specialists in optics and quantum radio physics.

UDC 621.378.33.001.5

COMPLEX GAUSSIAN BEAMS AS A MODEL OF NATURAL WAVES OF CAVITIES WITH TRANSVERSE OPTICAL INHOMOGENEITY

[Abstract of article by Ishchenko, Ye. F. and Ramazanova, G. S.]

[Text] It is shown that so-called complex gaussian beams are a more realistic model of cavity radiation than ordinary gaussian beams. Complex gaussian beams are the natural beams of spherical open resonators with gaussian (or weak quadratic) transverse variation of the transmission factor. A method of calculation is proposed, and the peculiarities of such beams are discussed. A comparison is made between theory and experiment.

UDC 539.184.001.5

RADIATIVE COLLISIONAL PROCESSES IN A SEMI-INFINITE PLASMA

[Abstract of article by Poddubnyy, L. I.]

[Text] The coefficient of braking absorption of neutral particles in collisions with ions and electrons is expressed in terms of correlation functions and calculated in the dipole approximation. The formalism of the density functional is used to describe radiation collisional processes at the surface of a simple metal. A direct variational principle is used to calculate the energy spectrum of the metal - atom system and the intensity of dipole transitions between the ground and excited states of the adsorbed atom.

UDC 535.2:531.19.001.5

STATISTICAL PROPERTIES OF A REFLECTED ELECTROMAGNETIC FIELD WITH COHERENT COMPONENT

[Abstract of article by Veklenko, B. A.]

[Text] The author studies the evolution of the radiation density matrix that determines the statistic of photocounts. The explicit form of the matrix is found for coherent radiation reflected from a half-space filled with quasiresonant atoms. The noise component is accounted for.

UDC 535.231.6:537.324

SENSITIVITY OF A SILICON HEAT SENSOR AS DEPENDENT ON RADIATION POWER

[Abstract of article by Aleksandrov, O. V., Barto, M. P., Vasil'yev, A. M., Mochalova, L. Yu. and Sharikhin, V. F.]

[Text] The paper examines the influence of various factors on linearity of the response of an absolute thermoelectric radiation power sensor. The considerable nature of the temperature dependence of heat losses from the sensing element is noted, especially convective-conductive losses. Experimental results are given.

UDC 535.2:531.19.001.5

CONCERNING THE QUESTION OF THE ADIABATIC HYPOTHESIS IN QUANTUM FIELD THEORY

[Abstract of article by Veklenko, B. A.]

[Text] It is hypothesized that assumption of a weakly noisy medium is sufficient for regularizing matrix elements (corresponding to disconnected diagrams in particular).

UDC 535.184.001.5

A METHOD OF CALIBRATING ABSOLUTE VALUES IN MEASUREMENT OF EXCITATION CROSS SECTIONS WITH THE USE OF EXTENDED INTERSECTING BEAMS

[Abstract of article by Smirnov, Yu. M. and Shapochkin, M. B.]

[Text] A method is described for calibrating excitation cross sections of transitions with respect to reference lines of the investigated substance or a reference gas. Errors of the calibration operation are analyzed in both cases.

UDC 535.318.001:535.811

THE METHOD OF 4 x 4 BEAM MATRICES IN PARAXIAL OPTICS

[Abstract of article by Reshetin, Ye. F.]

[Text] The method of 2 x 2 beam matrices that is well known in paraxial optics and is applicable only in calculating systems with certain symmetry elements is generalized to arbitrary optical systems by conversion to 4 x 4 matrices. A set of standard matrices is proposed that is sufficient for examining arbitrary piecewise-homogeneous optical systems with smooth interfaces. It is proved that any such system is equivalent in the paraxial approximation to some piecewise-homogeneous system with cylindrical boundaries.

UDC 535.8:532.517.4

INVESTIGATION OF THE TYPE OF KERNEL OF THE INTEGRAL EQUATION OF OPTICAL DOPPLER ANEMOMETRY

[Abstract of article by Krayneva, N. V., Kuznetsova, S. A. and Smirnov, V. I.]

[Text] An analysis is made of various cases of asymptotic expansion of the frequency-response function of an optical anemometer. It is shown that the type of kernel depends on the parameters of the reception and probing optics. The limiting case of tuning of the optical system corresponds to gaussian and lorentzian types of kernels, which is experimentally confirmed. The solution of the equation with gaussian kernel is of practical interest.

UDC 537.14:537.531.2

COHERENT CHANNEL OF UNDULATOR RADIATION

[Abstract of article by Grigor'yev, S. V.]

[Text] The paper examines the relation of coherent and incoherent channels of amplification of spontaneous radiation of relativistic electrons in an undulator. The quantum mechanical calculation of the coefficient of spontaneous emission is given where both channels are present. Conditions are found under which the coherent channel becomes appreciable.

UDC 537.14:537.531.2

EFFECT OF TRANSVERSE MOVEMENT OF ELECTRONS IN A BEAM ON AMPLIFICATION OF RADIATION IN AN UNDULATOR

[Article by Grigor'yev, S. V.]

[Text] An examination is made of the process of linear amplification of radiation in an undulator in the case of arbitrary velocity distribution of electrons of a beam injected into a resonator cavity. The quantum mechanical calculation of the amplification factor is presented. It is shown that the influence of transverse motion of the beam electrons on amplification is negligible in the case of nonzero detuning. In the case of zero detuning, the condition is found under which this motion becomes appreciable.

UDC 537.531.2

DIAGNOSIS OF AN ELECTRON BEAM IN A RAREFIED PLASMA FROM THE POLARIZATION-FREQUENCY AND STATISTICAL CHARACTERISTICS OF RADIATION

[Abstract of article by Gvozdovskiy, I. V. and Lebedev, A. K.]

[Text] The paper investigates the correlation of linear polarization of bremsstrahlung of a nonrelativistic monoenergetic plane beam of electrons with scattering by chaotically distributed potentials. It is shown that in a certain geometry the correlation of linear polarization is related in a simple way to beam divergence. The authors demonstrate the feasibility of following isotropization of beam electrons upon penetration into a plasma. An analysis is made of the evolution of the first moments of numbers of photons of different polarization.

UDC 541.182.65:535:628

ON THE FEASIBILITY OF USING A GEL OF Na-MONTMORILLONITE AS A CONTROLLABLE NEUTRAL LIGHT FILTER

[Abstract of article by Bliznyuk, V. V.]

[Text] It is experimentally established that when an alternating electric field with frequency of 100 kHz and intensity of up to 2000 V/m is applied to a gel of Na-montmorillonite, it behaves as a controllable neutral light filter. The observed effect is explained on the basis of consideration of multiple reflection from the interfaces between adjacent layers that are regions of identical orientation of the particles of the gel.

UDC 621.383.44:546.29.001.5

CHARACTERISTICS OF MDS STRUCTURES BASED ON CATHODE-SPUTTERED FILMS OF DIELECTRICS

[Article by Yermakov, B. V., Kozhevnikova, G. N., Spivak, V. S. and Sharikhin, V. F.]

[Text] The paper gives the results of an experimental study of MDS structures based on silicon using cathode-sputtered films of oxides of tantalum, zirconium, silicon and tin as the insulator. The values of the index of refraction are found for the films, the capacitance-voltage characteristics are measured, and the response of the MDS structure to optical radiation is determined.

UDC 537.14

CONCERNING NONLINEAR PROCESSES ACCOMPANYING TRANSITIONS IN THE CONTINUOUS SPECTRUM

[Abstract of article by Lebedev, A. K.]

[Text] The paper analyzes the semiclassical and quantum calculations of weakly nonlinear coefficients of bremsstrahlung upon adiabatic and instantaneous realization of interaction. These approaches lead to different expressions. However, the form of the saturation parameter is independent of the method of calculation,

and also of the kind of realization of the interaction. It is shown that if the state of the field of radiation is a superposition of states with different numbers of photons, the cross section of transitions in the quantum calculation agrees with the semiclassical approach.

UDC 539.186+539.107.5

EXPERIMENTAL INVESTIGATION OF EXCITATION FUNCTIONS USING A MULTICHANNEL PULSE ANALYZER

[Abstract of article by Malakhov, Yu. I.]

[Text] A report on using a multichannel pulse analyzer in a facility designed for studying processes of interaction of an electron beam with an atomic beam in the 5-300 eV electron energy range. Used as a multichannel pulse counter, the analyzer gives reliable measurements in the photon count mode, i. e. in the case of minimum concentration of atoms of the investigated substance. Data are accumulated and processed in a form convenient for computer input.

6610
CSO: 1862/178

UDC 548.539.21

NARROW-BAND TUNABLE OPTICAL FILTER BASED ON A $CdGa_2S_4$ SINGLE CRYSTAL

Moscow KVANTOVAYA ELEKTRONIKA in Russian Vol 8, No 4(106), Apr 81 pp 910-912

[Article by V. V. Badikov, I. N. Matveyev, S. M. Pshenichnikov, O. V. Rychik, N. K. Trotsenko and N. D. Ustinov]

[Text] A report on development of a polarization light filter that is temperature-tunable over a range of 487-580 nm. The filter is based on a $CdGa_2S_4$ single crystal and has a passband 2 nm wide with transmission of 48% at the maximum of the spectral characteristic combined with high resistance to laser radiation (32 MW/cm^2).

The solution of many problems of quantum electronics requires narrow-band tunable optical filters with high transmission in the band of transparency and resistance to laser radiation. Of considerable interest in this connection are light filters based on the selective isotropy and natural or artificial optical activity of some single crystals [Ref. 1]. A plate made from such a single crystal and placed between two polaroids in such a way that the optical axis of the crystal is parallel or perpendicular to the plane of polarization of the incident radiation is a narrow-band filter with maximum transmission at the point of isotropy, i. e. on the wavelength λ_0 on which birefringence is absent: $n_0(\lambda_0) = n_e(\lambda_0)$. Such filters are presently being made from binary compounds, among which are single crystals of CdS, CdSe, ZnO, Al_2O_3, ZnTe and others [Ref. 2-5]. However, they have a low transmission factor, a narrow tuning range, and require setting up artificial gyrotropy. Our research is devoted to development and experimental investigation of a narrow-band tunable light filter based on a single crystal of the ternary compound $CdGa_2S_4$. This crystal belongs to class $\overline{4}$, is transparent in the region of 0.48-13 μm, and has natural gyrotropy and a point of isotropy.

The $CdGa_2S_4$ single crystals were grown by the Bridgman-Stokebarger method. The initial elements Cd, Ga and S were put into a quartz ampule in stoichiometric proportions. The ampule was sealed under vacuum of about 0.1 μm Hg. The compound was synthesized in a two-zone horizontal furnace, after which the ampule containing the melt was transferred to a furnace for growing. The single crystals were grown at a rate of 14 mm per day. The single-crystal boules were 22 mm in diameter and 35 mm long. The optical quality of the single crystals was good, the specimens were homogeneous without internal twins or cords. Measurement of the absorption of the resultant specimens showed that it did not exceed 0.05 cm^{-1} in the entire

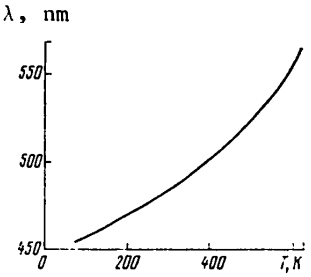

Fig. 1. Wavelength of isotropy as a function of temperature of $CdGa_2S_4$ crystal

visible band. Birefringence was measured by an interference method in which a plate of $CdGa_2S_4$ cut in direction <110> was placed between two crossed polaroids. The plane of polarization of radiation made a 45° angle with the optical axis of the crystal. The change in position of the point of isotropy as a function of the temperature of the crystal was measured by the same method, only the plate was placed in a thermostat with temperature regulation. The results of the measurements are shown in Fig. 1. As we can see, the region of temperature tuning of the point of isotropy covers the band of wavelengths from 450 to 580 nm. The position of the point of isotropy of a $CdGa_2S_4$ single crystal as a function of temperature in the range of 77-670 K is approximated by the expression

$$\lambda_0 = 1{,}737 \cdot 10^{-4} T^2 + 7{,}44 \cdot 10^{-2} T + 449,$$

where λ_0 is wavelength in nm, and T is temperature in K.

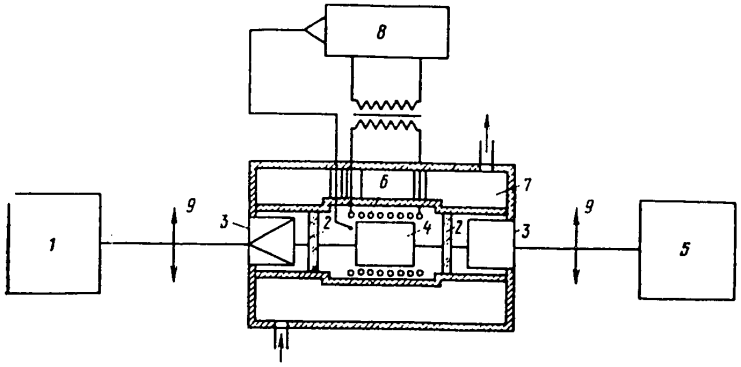

Fig. 2. Diagram of filter and experimental setup: 1--source of radiation; 2--input windows of the thermostat; 3--polarization prisms; 4--$CdGa_2S_4$ single-crystal plate; 5--receiver; 6--heating coil; 7--thermostat; 8--temperature regulator; 9--condensers

A diagram of the filter is shown in Fig. 2. It includes a single-crystal $CdGa_2S_4$ element 4 placed in thermostat 7, and two Arrens polarization prisms 3. The $CdGa_2S_4$ plate was cut in direction <110>, for which the temperature dependence of rotational capacity ρ_0 is minimum. The thickness d_0 of the plate was selected from conditions of maximizing the transmission, and was 7.8 mm. The light diameter of the filter was 20 mm. To eliminate convective flows of air, the heated volume was enclosed between two glass windows 2. For purposes of preventing heating of the external parts of the filter and for thermostatic control of the polarization prisms, the entire system was placed in a water-cooled jacket. The filter was tuned by varying the temperature in the thermostatic chamber over a range of 300-650 K by high-precision temperature controller 8 of the VRT-3 type. Measurements were made of the following filter parameters: spectral characteristic, half-width of the passband $\Delta\lambda$ with respect to level 0.5, transmission at the maximum

of the spectral characteristic τ, the degree of suppression δ--the ratio of transmission at the maximum of the spectral characteristic (0.5 μm) to transmission on a wavelength of 0.55 μm--tuning range (λ_{min}, λ_{max}), and resistance to laser radiation. The spectral characteristic of the filter at room temperature is shown in Fig. 3. The other measurements gave the following results: $\Delta\lambda = 1$ nm, $\tau = 48\%$, $\delta = 5 \cdot 10^{-5}$, $\lambda_{min} = 0.45$ μm, $\lambda_{max} = 0.58$ μm, power density of laser radiation at which the crystal was destroyed was $P_{max} = 32$ MW/cm^2 for $\lambda = 0.69$ μm and 68 MW/cm^2 for $\lambda = 1.06$ μm. We give for comparison the analogous parameters of a filter made of single-crystal CdS [Ref. 5]: $\Delta\lambda = 1$ nm, $\tau = 20\%$, $\lambda_{min} = 0.511$ μm, $\lambda_{max} = 0.522$ μm, range of temperature variation 77-300 K.

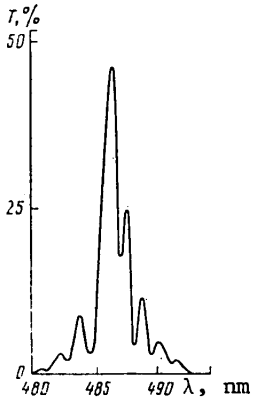

Fig. 3. Spectral characteristic of filter at room temperature

During tuning of the $CdGa_2S_4$ filter the spectral characteristic remained practically unchanged, and the transmission τ varied within limits of 5%, which was due mainly to the temperature dependence of rotational capacity ρ. It should be noted that the crystal was not subjected to antireflection treatment. Antireflection coating of the crystal will increase the transmission to 80%.

These studies have shown that a light filter based on a $CdGa_2S_4$ crystal has parameters that considerably surpass those of existing analogous filters.

REFERENCES

1. Hobden, M. B., ACTA CRYST., Vol A25, 1969, p 633.

2. Cobrecht, H., Bartchat, A., Z. PHYSIK, Vol 156, 1959, p 131.

3. Zil'bershteyn, A. Kh., Solov'yev, L. Ye., FIZIKA I TEKHNIKA POLUPROVODNIKOV, Vol 12, 1978, p 407.

4. Zil'bershteyn, A. Kh., Solov'yev, L. Ye., OPTIKA I SPEKTROSKOPIYA, Vol 35, 1973, p 471.

5. Laurenti, J. P. et al., REV. PHYS. APPL., Vol 12, 1977, p 1755.

6610
CSO: 1862/189

PLASMA PHYSICS

UDC 533.9+533.186+533.6.01

PLASMA PHYSICS, PHYSICS OF ELECTRONIC AND ATOMIC COLLISIONS, PHYSICAL GAS DYNAMICS

Leningrad FIZIKA PLAZMY, FIZIKA ELEKTRONNYKH I ATOMNYKH STOLKNOVENIY, FIZICHESKAYA GAZODINAMIKA in Russian 1978 (signed to press 22 Nov 78 pp 2-6, 62-63

[Annotation, introductory article and table of contents from book "Plasma Physics, Physics of Electronic and Atomic Collisions, Physical Gas Dynamics", edited by T. I. Soshkova, "Nauka", Leningradskoye otdeleniye, 2300 copies, 64 pages]

[Text] This pamphlet, relating to the sixtieth anniversary of the Physico-technical Institute imeni A. F. Ioffe of the USSR Academy of Sciences [FTI], surveys results found in the field of plasma physics, physics of electronic and atomic collisions, and physical gas and plasma dynamics in leading laboratories of the Institute for the last ten years. A brief history is given on development of research in this area.

Brief History of Research on Physics of Atomic Collisions and Plasma Physics

Research in the field of atomic collisions, i. e. interaction of atoms, molecules and their ions, was first started at FTI in 1948-1950 in the laboratory of V. M. Dukel'skiy. One of the problems was to study processes of ionization and charge exchange that accompany losses and capture of an electron in collisions of ions with atoms. The formulation of this problem was stimulated by the development of methods of electromagnetic separation of isotopes and analytical mass spectrometry, involving the creation of ion beams and compensation of the space charge of ions, and also the passage of such beams through a rarefied gas. Further development of research on the physics of collisions was determined both by problems of atomic physics, and by the need for data on elementary processes in the interaction of particles in rarefied ionized media--plasma and the upper atmosphere.

N. V. Fedorenko and his collaborators developed methods of analyzing the charge and mass of colliding particles. These methods enabled a transition from measurement of the total number of charged particles (electrons and ions) formed in collisions to investigation of the cross sections of processes with the participation of several atomic electrons, and with production of ions of different charges. In the late fifties, research series were done on a wide range of elementary processes accompanying atomic collisions, particularly processes in a high-temperature hydrogen plasma.

High-temperature plasma research was started at FTI in 1958 at the suggestion of I. V. Kurchatov in connection with expansion in the USSR of work on the problem of controlled nuclear fusion. This work was led by V. P. Konstantinov. Initially the main problem was to develop effective methods of studying (diagnosing) a hot

plasma. This task was extremely urgent since information on plasma parameters in different systems was incomplete and partly contradictory. Development of methods of plasma diagnosis was done at FTI in three major areas: corpuscular methods (V. V. Afrosimov's group, microwave methods (V. Ye. Golant's group) and optical methods (group under A. N. Zaydel'). The developed methods were tried out on the large Al'fa facility set up at the Scientific Research Institute of Electrophysical Equipemnt imeni D. V. Yefremov and investigated jointly by this institute and FTI. Later these methods began to be used on plasma facilities of FTI, on the plasma installations of the Institute of Atomic Energy imeni I. V. Kurchatov, the Physics Institute imeni P. N. Lebedev of the USSR Academy of Sciences and in other institutes.

Corpuscular methods of plasma research (N. V. Fedorenko, V. V. Afrosimov, M. P. Petrov, A. I. Kislyakov) are based on analysis of streams of particles emitted by the plasma ("passive diagnosis"), or on injecting beams of atomic particles into the plasma to determine the plasma parameters ("active diagnosis"). Among these techniques, the most widely used is corpuscular diagnosis based on streams of neutral particles, since these particles pass freely through electromagnetic fields used for plasma confinement, and may be analyzed outside the plasma facility. Passive plasma diagnosis, which was first suggested and realized at FTI, has become one of the major methods of utilizing the ionic component of a high-temperature plasma, and is in widespread use in the Soviet Union and elsewhere. This technique has enabled determination of the energy distributions of ions, analysis of energy losses by a plasma that are associated with corpuscular streams, and investigation of the nature of directional motion and drift of ions with reference to the anisotropy of such streams. Analysis of streams of fast atoms from a plasma has been found to be an extremely sensitive method of recording the instabilities that arise in a plasma. Active corpuscular diagnosis has turned out to be a quite effective method of studying ion concentration and electron temperature. Further development of these methods is directed toward the solution of the problem of measuring local plasma parameters.

Microwave methods of plasma research have been extensively developed at FTI (V. Ye. Golant, N. I. Vinogradov, A. I. Anisimov, V. A. Ipatov, M. M. Larionov, V. V. Rozhdestvenskiy et al.). Among the proposed methods, mention should be made first of all of the location method of determining the spatial distribution of electrons that has been extensively utilized in plasma experiments. There has also been considerable interest in a suggestion for using open cylindrical resonators to measure plasma concentration. FTI was the first to use passive microwave diagnosis on a large fusion facility. With the use of this facility, data on the electron temperature of the plasma on the Al'fa installation were obtained from data on the spectrum of microwave radiation. The same facility was used to do experiments on microwave scattering by turbulent plasma pulsations.

Spectroscopic methods of plasma research have been extensively used (A. N. Zaydel', G. M. Malyshev, Ye. Ya. Shreyder, A. B. Berezin et al.). A number of delicate spectroscopic methods have been developed. Among these, mention should be made of the determination of ion energy from Doppler broadening of spectral lines, investigation of collective movements with respect to Doppler shift, the study of impurities from radiation in the extreme ultraviolet, the isotope method of studying interaction of a gas with walls. Research has been started on developing and using a local method of measuring plasma density and temperature based on scattering of

laser radiation (G. M. Malyshev, G. T. Razdobarin et al.). The use of holographic methods of studying a dense plasma has been proposed, and development of such methods has been started (A. N. Zaydel', Yu. I. Ostrovskiy, G. V. Ostrovskaya).

In 1960, in addition to work on plasma diagnosis, experimental research was started on plasma phenomena, principally in two areas. The first has to do with investigation of plasma diffusion in a magnetic field (V. Ye. Golant, N. I. Vinogradov, D. G. Bulyginskiy et al.). The experiments resulted in determining the conditions of realization of classical diffusion caused by collisions, and ascertainment of the major characteristics of such diffusion. An investigation was also made of the way that diffusion is affected by turbulent fluctuations.

The second area is investigation of the interaction of high-frequency waves with a plasma (V. Ye. Golant, N. I. Vinogradov, A. D. Piliya, K. A. Podushnikova, O. N. Shcherbinin, M. M. Larionov et al.). During this same period, V. Ye. Golant, M. G. Kaganskiy et al. began development of facilities for studying adiabatic compression of a toroidal plasma. The investigation of these methods of heating and their use on fusion facilities of the tokamak type subsequently became one of the major areas of laboratory research.

In the early sixties work began on plasma containment in complex closed magnetic fields. Based on theoretical studies of the topology of magnetic fields (G. V. Skornyakov), a trap was developed and plans were started on the Tornado Project in which research is still developing (B. P. Peregud, V. M. Kuznetsov, A. A. Semenov et al.). In recent years this work has been done jointly with the Swedish Academy of Sciences.

Contents page

6610
CSO: 1862/185

THERMODYNAMICS

UDC 536.2:536.7:621.1

HEAT CONDUCTION AND CONVECTIVE HEAT EXCHANGE

Kiev TEPLOPROVODNOST' I KONVEKTIVNYY TEPLOOBMEN in Russian 1977 (signed to press 24 Aug 77) pp 2, 124-125

[Annotation and table of contents from book "Heat Conduction and Convective Heat Exchange", edited by V. A. Bulkina, Institute of Technical Thermophysics, UkSSR Academy of Sciences, Izdatel'stvo "Naukova dumka", 500 copies, 136 pages]

[Text] The collection contains materials of the Seventh Scientific and Technical Conference of Young Scientists of the Institute of Technical Thermophysics, UkSSR Academy of Sciences, held in Kiev, April 1976. Results are given from theoretical and experimental research in the field of heat conduction and convective heat exchange of one-phase and two-phase media. An investigation is made of some aspects of the stochastic theory of transport, approximate solutions are given for some linear and nonlinear problems of heat conduction, research results are given on heat exchange in the case of laminar and turbulent flows of one-phase and two-phase fluids in pipes and channels.

The book is intended for scientific and technical-engineering personnel in the field of heat and mass exchange, and also for undergraduate and graduate students majoring in appropriate fields.

Contents

6610
CSO: 1862/172

END